SANDIA REPORT

SAND2015-0179
Unlimited Release
January 2015

A Performance Model for Photovoltaic Modules with Integrated Microinverters

Daniel Mark Riley
Clifford W. Hansen
Michaela Farr

Prepared by
Sandia National Laboratories
Albuquerque, New Mexico 87185 and Livermore, California 94550

Sandia National Laboratories is a multi-program laboratory managed and operated by Sandia Corporation, a wholly owned subsidiary of Lockheed Martin Corporation, for the U.S. Department of Energy's National Nuclear Security Administration under contract DE-AC04-94AL85000.

Sandia National Laboratories

Issued by Sandia National Laboratories, operated for the United States Department of Energy by Sandia Corporation.

Available to DOE and DOE contractors from
U.S. Department of Energy
Office of Scientific and Technical Information
P.O. Box 62
Oak Ridge, TN 37831

Telephone: (865) 576-8401
Facsimile: (865) 576-5728
E-Mail: reports@adonis.osti.gov
Online ordering: http://www.osti.gov/bridge

Available to the public from
U.S. Department of Commerce
National Technical Information Service
5285 Port Royal Rd.
Springfield, VA 22161

Telephone: (800) 553-6847
Facsimile: (703) 605-6900
E-Mail: orders@ntis.fedworld.gov
Online order: http://www.ntis.gov/help/ordermethods.asp?loc=7-4-0#online

SAND2015-0179
Unlimited Release
January 2015

A Performance Model for Photovoltaic Modules with Integrated Microinverters

Daniel Riley, Clifford Hansen, Michaela Farr
Photovoltaic and Distributed Systems
Sandia National Laboratories
P.O. Box 5800
Albuquerque, New Mexico 87185-MS0951

Abstract

Photovoltaic (PV) systems using microinverters are becoming increasingly popular in the residential system market, as such systems offer several advantages over PV systems using central inverters. PV modules with integrated microinverters, termed AC modules, are emerging to fill this market space. Existing test procedures and performance models designed for separate DC and AC components are unusable for AC modules because these do not allow ready access to the intermediate DC bus. Sandia National Laboratories' Photovoltaics and Distributed Systems department has developed a set of procedures to test, characterize, and model PV modules with integrated microinverters. The resulting empirical model is able to predict the output AC power of with RMS error of 1-2%. This document describes these procedures and provides the results of model validation efforts.

CONTENTS

FIGURES

TABLES

NOMENCLATURE

AC	Alternating current
AOI	Angle of incidence
DC	Direct current
DNI	Direct normal irradiance
DOE	Department of Energy
IEC	International Electrotechnical Commission
MBE	Mean bias error
POA	Plane of array
PV	Photovoltaic
RMSE	Root mean square error
SNL	Sandia National Laboratories

1. INTRODUCTION

The use of microinverters in photovoltaic (PV) systems has increased greatly over the past seven years. There are many benefits which microinverters bring to PV system planning. The use of microinverters removes the necessity to attempt to match the DC current through each PV module in a string of modules, thus allowing more flexibility regarding module placement and orientation. Systems with microinverters typically operate at 240 or 480 AC volts, while systems with central inverters operate at up to 600 or 1000 DC volts; this reduction in voltage improves the safety of the system and reduces the risk of arc faults, which are the leading source of fires caused by PV systems.

Typically, microinverters are distinct components in a PV system. Thus, the PV modules and the inverters may be characterized separately and system output can be modeled using combinations of existing models [1-4]. Some manufacturers are fully integrating a microinverter into a PV module, combining the separate elements into a single unit termed an AC module, which is defined as a PV module with fully integrated inversion electronics. In an AC module, there is no ready access to the DC portion of the circuit. The AC module is a product which accepts incoming irradiance and produces only AC power [5].

Without access to the DC portion of the circuit, and without the ability to separate the PV module from the inversion electronics, it is impossible to characterize the PV module and the microinverter separately, which prevents application of existing performance models to AC modules. If we assume that AC modules will become significant in the PV system marketplace, then there is a need for methods to compare AC module performance and to predict their power generation.

To that end, Sandia National Laboratories has developed methods to characterize the performance of an AC module and an empirical performance model for AC modules. The model predicts the active AC power which an AC module should generate as a function of absorbed plane of array (POA) irradiance, airmass, air temperature, and wind speed.

This report describes the development of the AC module performance model. Section 2 presents the performance model and how it may be operated. Section 3 describes the various outdoor test procedures which must be performed to gather data about the performance of the AC module under test. Section 4 provides the analysis methods to transform the test data into model parameters. Finally, Section 5 shows the performance of the model by comparing model predictions to measured data.

2. MODEL DESCRIPTION

Sandia National Laboratories has developed an empirical performance model for AC modules. The model is predicts the active AC power of the AC module as a function of environmental inputs and/or operating conditions. As such, the primary model is an electrical power model, however, the electrical power model requires inputs from several sub-models. The electrical model's functional form is a piecewise continuous function with three subdomains. Each subdomain represents an operational state of the inversion electronics present within the AC module.

We suggest here a number of potential sub-models and explain their purpose within the primary electrical model. We have selected these submodels for their simplicity and accuracy; however, other submodels exist which may be used as alternatives.

2.1. Electrical Power Model

We have simplified the general operation of an AC module into three operational states; the low-irradiance state, the self-limiting state, and the typical operation state. The output power of an AC module is determined by the performance of the module within its current state.

2.1.1. Model for Low Irradiance State

The AC module operates in the low-irradiance state when there is insufficient irradiance to power the inversion electronics. In the low-irradiance state, the AC module may consume a small amount of power drawn from the electrical grid. The power produced in this state, P_3, is determined by equation 1:

$$P_3 = -1 \times P_{NT} \quad \textbf{(1)}$$

where P_{NT} is the consumed power in watts (frequently called the "night tare" power). P_{NT} may be obtained from specification sheets or may be determined empirically. Equation 1 may be modified if the low-irradiance power consumption is found to be a function of other inputs (e.g. temperature); however, it is generally reported as a single value. Note that the value of P_3 is negative to indicate that the AC module consumes power in the low-irradiance state.

2.1.2. Model for the Self-Limiting State

The inverters within AC modules, like centralized PV inverters, generally have some output power level at which they begin to limit their output. This is commonly known as "clipping". In order to accurately predict the output power of an AC module, this self-limiting level must be known. The power produced in this state is P_2 as determined by equation 2.

$$P_2 = P_{AC,max} \quad \textbf{(2)}$$

We have chosen to show the self-limiting power of the AC module as a constant value equal to the maximum active power output. The value of $P_{AC,max}$ may be reported on a specification

sheet, but we recommend determining this value empirically because reported values, in our experience, may be inaccurate for some AC modules.

While the self-limiting power output of the AC module may actually change with other input variables (e.g. ambient temperature, irradiance, air pressure), we suspect that these changes are much lower order effects. However, if the modeler has additional information to describe the self-limiting power as a function of other variables, a more general function indicated by equation 3 may be used.

$$P_2 = f(P_{ACmax}, T_{ambient}, E, \dots) \quad \textbf{(3)}$$

2.1.3. Model for the Typical Operation State

In the typical operation state, the AC module is operating normally without self-limiting its output. The power output of the AC module varies with changes in irradiance, cell temperature, and airmass as is described in equation 4. In the typical operation state, the module AC power output is represented as the product of a reference power and a series of scaling factors which modify the reference power. These scaling factors are themselves functions of absolute airmass (used as an easily calculated proxy for spectrum [6]), PV cell temperature, and incident irradiance. Prior experiments have determined that the temperature of the inversion electronics do not have a strong influence on the power generation, and thus the inverter temperature has been omitted [7].

$$P_1 = Pac_{ref} \times f_1(AMa - AMa_{ref}) \times \left[C_0 \times \frac{E_{POA}}{E_{ref}} + C_1 \times \ln\left(\frac{E_{POA}}{E_{ref}}\right)\right] \times \left[1 + \gamma_{ac}(T_c - T_0)\right] \quad \textbf{(4)}$$

where:

Pac_{ref} is the AC power under reference conditions E_{ref}, AMa_{ref}, and T_0, (W)

f_1 is an empirical unitless function which modifies the output power as a function of absolute airmass relative to the reference airmass

AMa is the absolute (pressure corrected) airmass, (unitless)

AMa_{ref} is the reference airmass condition, which may not necessarily be 1.5

C_0 is a unitless empirical coefficient describing the linear relationship between the irradiance and the power, typical values near 1

C_1 is a unitless empirical coefficient describing the logarithmic relationship between the irradiance on the power

E_{POA} is the broadband POA irradiance incident upon the module which reaches the active PV material, (W/m^2). E_{POA} is estimated from measured broadband POA irradiance by accounting for the module losses due to specular reflection and/or acceptance of diffuse irradiation .

E_{ref} is the reference POA irradiance, (W/m^2)

γ_{ac} is the response of the AC module's power output to change in cell temperature in units of 1/°C, referenced to T_0

T_c is the cell temperature of the AC module, (°C)

T_0 is the reference cell temperature of the AC module, usually 25 °C

With the performance of each state thus defined, it is a simple matter to determine the operating state of the AC module by comparing the power output calculated for each state. As shown in equation 5, the AC power for the typical operation state P_1 is calculated and compared to P_2 and P_3 to determine P_{AC}, the active AC power at each time .

$$P_{AC} = \begin{cases} P_1 & if \quad P_3 \le P_1 \le P_2 \\ P_2 & if \quad P_1 > P_2 \\ P_3 & if \quad P_1 < P_3 \end{cases} \tag{5}$$

In practice, it is most difficult to predict the power output of an AC module system which is operating in the typical operation state and governed by power P_1. For this reason, we have formulated the equation for P_1 as a product of factors with terms that are normalized to a reference power condition. The normalized terms make the equation "modular" in nature, and where better information is available, the expression may be replaced by a more complex expression which more accurately represents the AC module's operation. For example, if it is known that the operating power of an AC module system is affected by inverter temperature, an inverter temperature adjustment may be incorporated with the cell temperature adjustment. We hope that such flexibility allows the model to be easily modified for improved accuracy.

2.2. Sub-Models

Eq. 4 requires the use of additional sub-models to determine several of its factors. For example, a cell temperature model may be used to estimate cell temperature, and an angular losses model may be used to estimate the fraction of irradiance reaching the cell as a function of solar angle of incidence (AOI).

2.2.1. Cell Temperature Model

If cell temperature is not measured, it may be determined by the use of a cell temperature model such as those described in [1,8,9]. The electrical model does not require the use of any particular cell temperature model.

For the sake of simplicity we present the cell temperature model described in [1] in equations 6 and 7. This particular model determines average module temperature from wind speed, ambient temperature, irradiance, and a pair of empirically derived coefficients, then determines the average cell temperature from the average module temperature, irradiance, and temperature difference between the cell and module. This particular model is intended to be used when the module is in thermal equilibrium (i.e. the module is not heating up or cooling down).

$$T_m = E \times \left(e^{a+b\times WS}\right) + T_a \tag{6}$$

$$T_c = T_m + \frac{E}{E_0} \times \Delta T \tag{7}$$

where:
T_m is the average module back-surface temperature, (°C)
E is the solar irradiance incident on the module surface, (W/m^2)

WS is the wind speed measured at a standard 10 meter height, (m/s)
a is an empirically determined coefficient establishing the upper limit for module temperature at low wind speeds and high solar irradiance
b is an empirically determined coefficient establishing the rate at which module temperature drops as wind speed increases
T_a is the ambient air temperature, (°C)
E_0 is the reference solar irradiance on the module, typically 1000 W/m^2
ΔT is the temperature difference between the cell and the module back surface at an irradiance level of E_0, typically 3 °C for flat-plate modules on an open rack.

2.2.2. Airmass sensitivity model

Since the current produced by the DC component of an AC module changes as a function of the spectrum of incident light, the AC power of the module also changes. The performance model includes the empirical function f_1 to represent this effect. Changes in absolute (pressure corrected) airmass are highly correlated with changes in spectrum during clear-sky periods. Furthermore, absolute airmass is easily calculated as a function of sun elevation [10] and subsequent application of a correction factor for the site pressure [11]. Here, we employ a third order polynomial to describe the variation in power as a function of absolute airmass as shown in equation 8. However, we note that in order for the f_1 function accurately represent the change in AC power, the POA irradiance data used for model predictions must be obtained using a sensor with a similar spectral response to the sensor which was used to calibrate the f_1 function (see Section 4.5); alternatively, spectral corrections should be made to the POA irradiance data.

$$f_1\left(AMa - AMa_{ref}\right) = 1 + A_1 \times \left(AMa - AMa_{ref}\right) + A_2 \times \left(AMa - AMa_{ref}\right)^2 + A_3 \times \left(AMa - AMa_{ref}\right)^3 \quad \textbf{(8)}$$

2.2.3. Incident Angle Modifier Model

The broadband POA irradiance incident upon an inclined surface is comprised of both direct and diffuse components; and the direct component of the irradiance is proportional to the cosine of the solar AOI as shown in equation 9.

Flat plate PV modules do not exhibit perfect cosine response to the incident angle of direct irradiance. The ratio between the direct irradiance reaching the module's cells (E_{POA}) and the direct irradiance incident on the module's surface (E_b) can be described as a function of AOI, $f_2(\theta)$, which has the range of 0 to 1. Usually, for incident angles (θ) between 0° and 50° f_2 remains at 1, indicating that a constant proportion of the beam irradiance incident upon the module is transmitted to the PV cells. At higher incidence angles, however, the air/glass interface causes specular reflections and the value of f_2 begins to drop toward 0.

Several models have been proposed to characterize these reflection losses [1, 12-14]. Any of these model forms may be used (with more or less accuracy according to the model). We suggest using the model described by Martin and Ruiz in [14] to act as the f_2 function which modifies the beam component of E_{POA} as shown in equation 10. The model form proposed by Martin and

Ruiz has the advantages of being a simple model with only a single parameter and is monotonically decreasing with increasing solar AOI.

$$G_{POA} = E_b + E_{diff} = E_{DNI} \times \cos(\theta) + E_{diff} \quad \textbf{(9)}$$

$$E_{POA} = E_b \times f_2(\theta) + E_{diff} = E_{DNI} \times \cos(\theta) \times \frac{1 - e^{\left[\frac{-\cos(\theta)}{a_r}\right]}}{1 - e^{\left(\frac{-1}{a_r}\right)}} + E_{diff} \quad \textbf{(10)}$$

where:
G_{POA} is the total broadband plane of array incidence, (W/m^2)
E_{diff} is the diffuse plane of array irradiance, (W/m^2)
θ is the solar AOI
E_{DNI} is the direct normal irradiance, (W/m^2)
E_b is the beam component of the sunlight incident upon the plane of array, defined as $E_{DNI} \times \cos(\theta)$, (W/m^2)
a_r is an empirically defined angular loss coefficient as defined in [14]

This form of determining E_{POA} is specifically meant for modules which produce power from direct irradiance and diffuse irradiance in the same proportion (i.e. the power production is insensitive to the diffuse or direct nature of the incident irradiance), as is the case in most flat-plate PV modules. If the AC module produces less power from diffuse irradiance than direct irradiance, as in concentrated PV modules, the diffuse irradiance may be modified as in [1] with another coefficient.

Equation 10 requires direct normal irradiance (DNI) and diffuse POA irradiance. When measurements of these quantities are not available, various other models may be used to estimate DNI and diffuse POA irradiance, e.g., [15-24]. Measured POA irradiance may be used in equation 10 if the measurements are adjusted for differences between the reflection losses of the irradiance sensor and those of the AC module. These models are not the subject of this paper, but we acknowledge that they may be required for practical operation of the model.

2.3. Practical Considerations of Model Operation

Due to the model form for the typical operation state, there are some practical considerations which must be addressed in order for the model to accurately predict the power of the AC module.

2.3.1. Incident Irradiance less than or equal to 0

The irradiance incident upon an AC module will fall to 0 W/m^2 during the night and radiative cooling during these periods may produce measured irradiance less than 0 W/m^2. However, if an incident irradiance less than or equal to 0 is applied in equation 4, attempting to take the logarithm of the normalized irradiance will yield an incorrect result. We therefore recommend that all values of E_{POA} be limited to a minimum of 0.1 W/m^2 prior to evaluation of equation 4.

This minimum value should yield a power which is less than P_3, the low-irradiance power output.

2.3.2. Extreme values of f_1 function

Due to the polynomial nature of the suggested f_1 function, it is possible that large values of AMa may generate a value for f_1 which is unrealistically large or small. We typically find that f_1 values are usually reasonable out to absolute airmasses of 10-12 (at which time the sun is likely very close to the horizon), but we suggest that modelers examine the possible values of f_1 and limit the maximum and minimum value of f_1 to values which are realistic.

3. TEST PROCEDURES AND EQUIPMENT

In order to generate the model parameters which describe the performance of an AC module, a series of tests must be conducted to measure the performance while varying the operating conditions of the AC module. This section lists a set of necessary equipment and measurements which must be made during this testing, as well as describing the test procedures. Unlike standard DC modules that can be tested indoors on a flash simulator, AC modules require a constant light source and must either be tested outdoors or under a continuous solar simulator. This paper only covers outdoor testing methods.

3.1. Equipment and Measurements

The testing requires the following signals be measured simultaneously and recorded. Equipment necessary to make these measurements is therefore also required. The sample rate of the data acquisition system may vary depending on the type of test performed, therefore, sample rates are suggested in the sections regarding those particular tests.

- Absolute time
- Direct normal irradiance via broadband pyrheliometer
- Plane of array irradiance via broadband pyranometer with good cosine response, must be coplanar with the AC module
- Wind speed, measured at a 10 meter height
- Ambient (dry bulb) temperature
- Average module temperature, preferably by no fewer than 3 thermocouples on module backsheet arranged per IEC 61853
- Active AC power produced or consumed by the AC module
- Solar AOI between module normal and sun, may be calculated

Additionally, a 2-axis solar tracker is required. The tracker must be capable of varying the solar AOI between 0 and 85 degrees and should also be capable of tracking the sun to within 5 degrees of the horizon.

The 2-axis tracker is required to determine the reflection losses (i.e., the empirical function f_2) and its use throughout the module characterization process will yield the most accurate results. If, however, the empirical function f_2 is known or is determined by some other means, it may be possible to determine the other model parameters in a manner similar to methods for calibrating performance models for DC modules using data collected during outdoor operation on fixed-tilt racking [25, 26]. We have not yet applied these methods to the characterization of AC modules.

3.2. Electrical Performance Test

The purpose of the electrical performance test is to measure the AC module system performance under a variety of irradiance, solar spectrum, and temperature conditions. The test seeks to fix the solar AOI to 0° in order to remove effects from varying incident angles.

3.2.1. Electrical Performance under Lighted Conditions

The electrical performance test is performed by mounting the AC module system on the 2-axis tracker and tracking the sun to achieve a constant 0° AOI. During the test, all required signals in Section 3.1 must be measured periodically at a rate no less than once every 30 seconds. All signals should be measured nearly simultaneously, with measurements of all signals occurring within 5 seconds of each other.

Electrical performance measurements should be performed until the module has been measured during a wide range of irradiance and weather conditions. It is most important to obtain measurements over a range of irradiance and airmass conditions. Of course, it is preferable to obtain the largest possible range of operating conditions during testing in order to represent these conditions in regressions that generate model parameters; however, we realize that resource constraints may make it impractical to have a single module under test for a very long time. The following irradiance and airmass ranges should be observed:

- Plane of array irradiance range which at least spans 200 to 1000 W/m^2
- Absolute (pressure corrected) airmass range spanning at least airmass 1.5 to airmass 5 under clear-sky conditions (no clouds within 20° of the sun)

We further recommend monitoring the AC module performance over a range of ambient air temperature and wind speed (which affects module temperature) conditions, although we do not believe the ranges of temperature and wind speed to be as critical as ranges of irradiance and airmass. Therefore, the following ranges are highly recommended:

- Wind speed range up to 7 m/s
- Ambient air temperature range greater than 15 °C

3.2.2. Electrical Performance under Dark Conditions

Lastly, electrical performance must be measured under extremely low light conditions. This may be achieved by measuring the active AC power of the module at night, while the module is in a dark room, or while the PV material is completely obscured with an opaque cover. It is not necessary to achieve a wide range of weather conditions (temperature, wind speed, etc.) when measuring the performance under dark conditions.

3.3. Transient Thermal Test

The purpose of the transient thermal test is to determine the AC module's response to changing temperature. The test operates the AC module system over a range of temperature conditions while solar irradiance and spectrum are nearly constant.

There may be several methods of ensuring a range of operating temperatures under nearly constant irradiance and spectral conditions including methods such as forced heating or cooling. However, Sandia National Laboratories typically shades the module with an opaque cover to allow the module to cool to near-ambient temperature, then un-shades the module to allow the

solar radiation to heat the module. The procedural requirements explained in this section are specific to this method of cooling/heating, and other requirements may be necessary if a different cooling/heating method is used.

In order to conduct transient thermal testing in the same fashion as Sandia National Laboratories, transient thermal testing must occur on clear sunny days, preferably within 45 minutes of solar noon in order to limit the variation in POA irradiance and spectrum over the duration of the test.

The module is mounted on the two-axis solar tracker to track the sun. Ideally, the module would be tested with a 0° AOI and operate in the "typical operation" state. However, in some cases, the AC module may operate in the self-limiting state (i.e. "clipping" its output) when under a 0° AOI. In the case where the module operates at the self-limiting state at 0° AOI, the solar tracker should be oriented and moved throughout the test to maintain a constant non-zero AOI for the test duration. The non-zero AOI should be selected to provide the highest POA irradiance while still allowing the module to avoid the self-limiting state. In cases where a non-zero AOI must be used, we recommend that the AOI be less than 40° in order to reduce light reflections from the air/glass interface. Alternative methods to reducing POA irradiance may also be used (e.g. shading screens) so long as the reduced irradiance is measured.

The module is covered with an opaque cover, mounted approximately 5 cm from the module's front surface such that none of the module's PV cells are illuminated by direct light and the vast majority of diffuse light is occluded by the shade. Module temperatures are monitored as the module cools to near-ambient temperature. Once the module and inverter are within approximately 5 °C of ambient temperature, the opaque shade material shall be removed and the module allowed to heat to operating temperature. Measurements should be taken as quickly as possible, with no less than a 0.1 Hz measurement frequency. We recommend a 1 Hz measurement frequency during the transient thermal test.

The time required for the system to come to operating temperature may vary based upon the module construction, but testing by Sandia indicates that some PV modules and inverters may heat to operating temperature in 30-60 minutes. The change in PV module temperature using this method is usually in the range of 20° to 30° C. POA irradiance variation during the test should be less than 2%. Furthermore, we recommend performing the transient thermal testing while wind speeds are less than 4 m/s in order to improve temperature uniformity across the module.

3.4. Inverter Response Time (Optional)

While it is not present in the performance model for AC modules, it *is* possible to measure the time required for the AC module to response to a large change in incident irradiance.

The transient thermal test procedure, applying and then removing an irradiance shade, causes a large change in irradiance incident on the module. If a fast-response irradiance measurement instrument (e.g. a photodiode or PV cell) is mounted near the AC module and covered/uncovered at the same time as the AC module, the irradiance instrument's response will indicate the time at which the module was uncovered.

After the AC module is uncovered, the inversion electronics must begin the process of finding the maximum power point of the PV module's current-voltage (I-V) curve. Once the output power of the AC module has stabilized, the maximum power point has been found and the AC module is operating normally. The time between the uncovering of the AC module and the stabilization of the output power is a measurement of how quickly the inversion electronics can correctly maximum power point track the PV module.

In Figure 3, the AC module was uncovered at time marker 540, and the AC module reached maximum power approximately 5 seconds later. Sandia's testing of two microinverters suggests that the MPPT times for commercial microinverters can be very short, on the order of 2-5 seconds, and therefore a high rate of data acquisition is required.

3.5. Angle of Incidence Test

Angle of incidence testing allows for characterization of the AC module's response to solar AOI. The AOI test varies the solar AOI while the direct and diffuse irradiance are nearly constant. The goal of the AOI test is to generate data which can be summarized by the f_2 function in equation 10. Since varying the solar AOI changes the POA irradiance, the PV module temperature also varies and these effects must be corrected using information from the transient thermal test.

While it is possible (and much simpler) to calculate E_{diff} from measured values of G_{POA}, E_{DNI}, and θ, we believe that it is preferable to measure the value of E_{diff} directly from a pyranometer in the plane of the 2-axis tracker and calculate $G_{POA}$from E_{DNI}, E_{diff}, and θ. In cases where it is possible to measure E_{DNI}, E_{diff}, and θ; the in-plane global irradiance should be calculated from these measured parameters and the measured in-plane global irradiance should be ignored. We suspect that in most cases, it will not be convenient to measure E_{diff}, and it will therefore be calculated from measured values of E_{DNI}, θ, and G_{POA}.

Angle of incidence testing must be performed on a clear-sunny day, preferably within 45 minutes of solar noon, in order to limit the variation in irradiance and spectrum during the test. The module is mounted on the solar tracker and begins the test with a 0° solar AOI.

One goal in designing an AOI test is to minimize the duration of the test; in order to limit changes in irradiance, spectrum, and module temperature. We again note that in some cases, the PV module may be oversized relative to the inverter which causes the inverter to limit the power output of the module (known colloquially as 'clipping'). If power limiting occurs at 0° solar AOI near solar noon, it is necessary to begin the test before or after solar noon at a time when self-limiting does not occur (under clear-sky conditions).

The module should begin the test with a 0° solar AOI, then the module should be rotated away from the sun in a series of movements with known AOI. The AC module should be measured at AOI=0 for at least 10 measurements in order to establish a baseline performance. We recommend briefly holding the module at each nonzero AOI in order to measure the performance of the AC module system at that solar AOI. Sandia uses stops that are approximately 5° apart in AOI and allows 30-90 seconds to elapse at each stop. There is no prescription for measurement

frequency during this test, but as the tests are (ideally) short we recommend sampling as quickly as possible. Sandia uses a 1 Hz measurement frequency during AOI tests.

Sample data from a Sandia AOI test are shown in Figure 1.

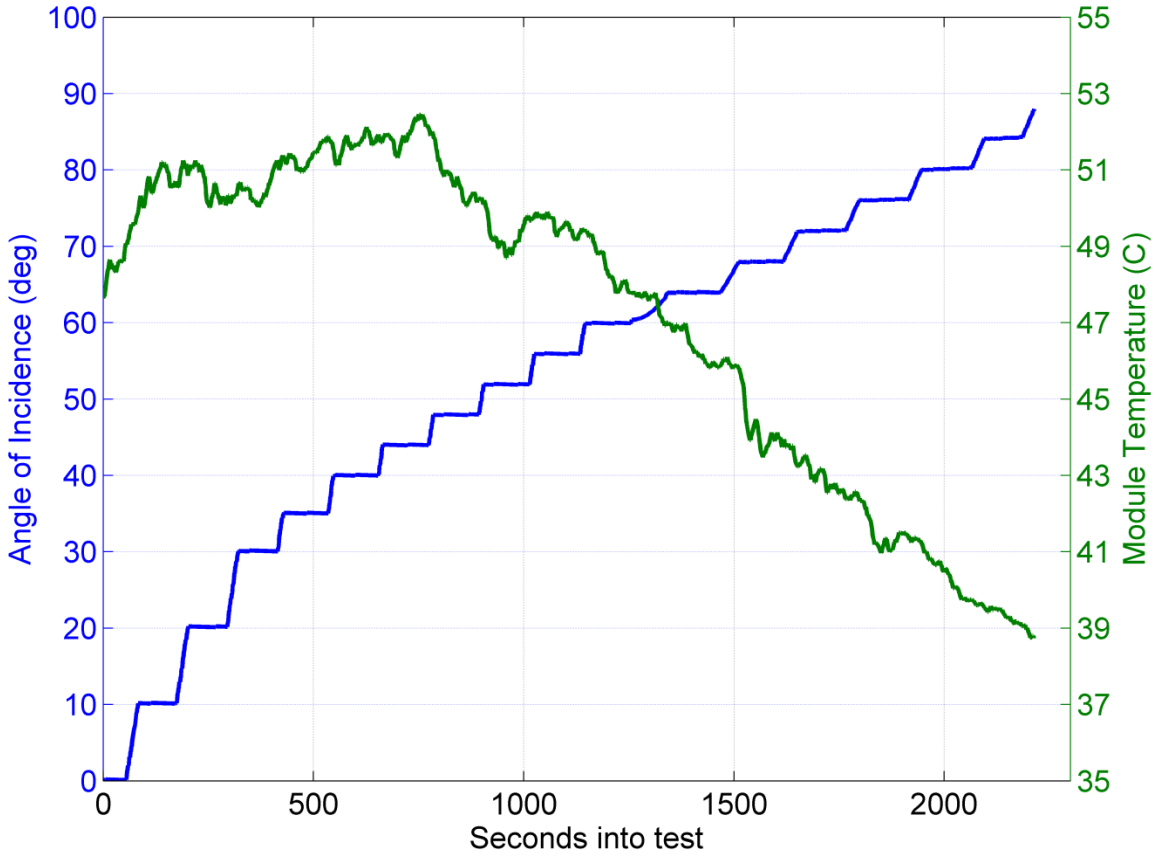

Figure 1: Sample data from an AOI test

4. PARAMETER DETERMINATION

After the testing specified in Section 3 is complete, the data are used to obtain values for the parameters of the performance model. In section 4, we present the process for analyzing the test data to determine parameters for the AC module model. Section 4.1 describes determination of the temperature coefficient from the transient thermal test data. Sections 4.2 through 4.7 describe determination of most parameters in the electrical performance model from the electrical performance test data, and Section 4.8 describes determination of the reflection loss function f_2 from the AOI test data.

We note that it may be difficult to develop accurate model parameters for some AC modules, in particular, for AC modules which begin to self-limit their output power at very low irradiance levels. For such modules it may be easy to observe the self-limiting state, but difficult to measure performance in other states, which may lead to less accurate models.

4.1. Determining the Temperature Coefficient

The temperature coefficient quantifies the effect of operating temperature on the AC power output of the system. As noted in [7], the temperature of the PV module has a much greater impact on the performance of the AC module than the temperature of the inverter. As such, it is appropriate to simplify the temperature of the AC module system by measuring only the module temperature.

The temperature coefficient of the AC module system, γ_{ac}, can be determined from data in the transient thermal test. We note γ_{ac} is a normalized temperature coefficient (i.e. it has units of 1/°C), thus γ_{ac} must be generated and subsequently implemented with the same reference temperature, T_0.

The first step in determining the temperature coefficient is to select data gathered during the thermal test. The test data may need to be reduced in order to find the period of time where the module temperature was increasing. As shown in Figure 2, the mean back surface temperature of the PV module increased from approximately 29 °C to 50 °C after removal of the opaque cover during the transient thermal test. The module temperature then moved within the range 50 °C to 60 °C for approximately 45 minutes. For the analysis to determine the temperature coefficient of the AC module system, only the data during the initial temperature rise is selected.

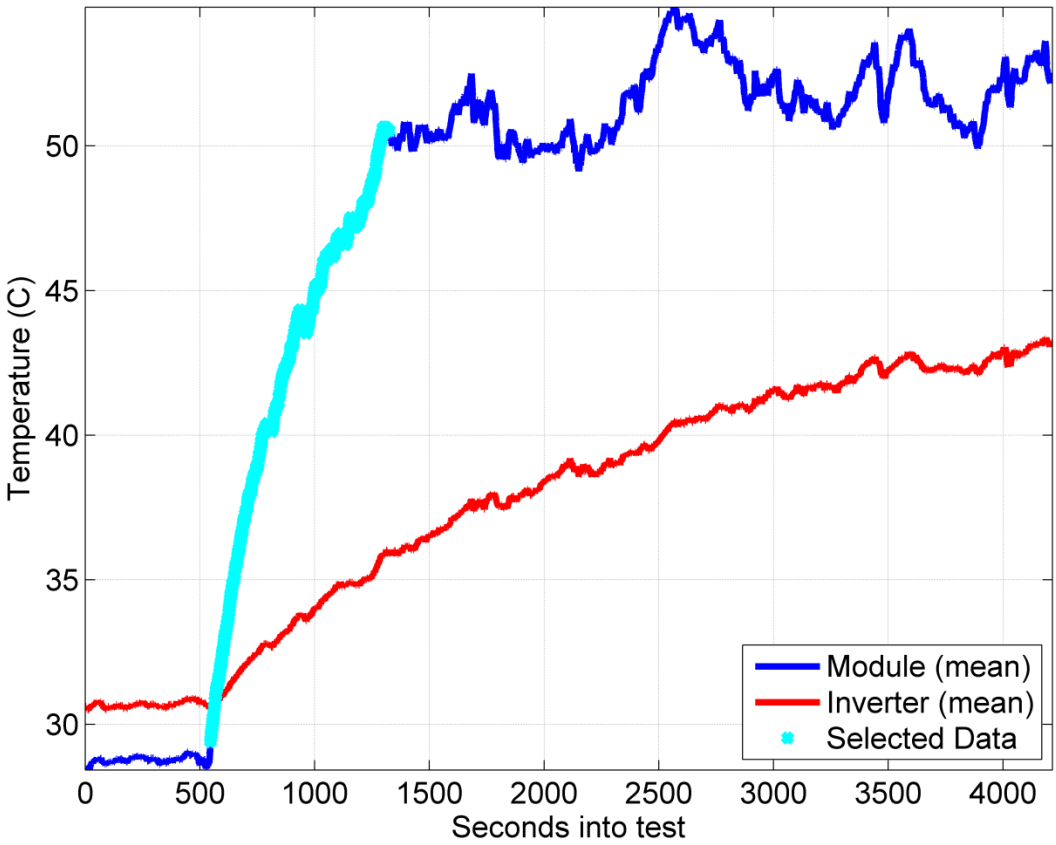

Figure 2: Component temperatures during transient thermal test and data selected for analysis

The second step in determining the temperature coefficient is determination of a reference irradiance and power to which future power measurements may be normalized. Figure 3 shows a plot of the data as the opaque cover was removed at 540 seconds. The AC module reaches its operating point within about 4-5 seconds of removal of the cover. A short period of time (less than 30 seconds) after the module has reached its operating point, the thermal reference irradiance and thermal reference power may be selected by the analyst; in the case of Figure 3 they are 1091 W/m^2 and 178.1 W, respectively. Note that these values are *not* E_{ref} and Pac_{ref} from equation 4. Rather, they are reference values only for use in determining the temperature coefficient which we denote as $E_{0,therm}$ and $P_{0,therm}$.

Because we have not yet established the response of the module to varying irradiance, we assume that irradiance and output power have a linear relationship over the small irradiance range around $E_{0,therm}$ which occurs during the transient thermal test (irradiance changes during the test are 2% or less).

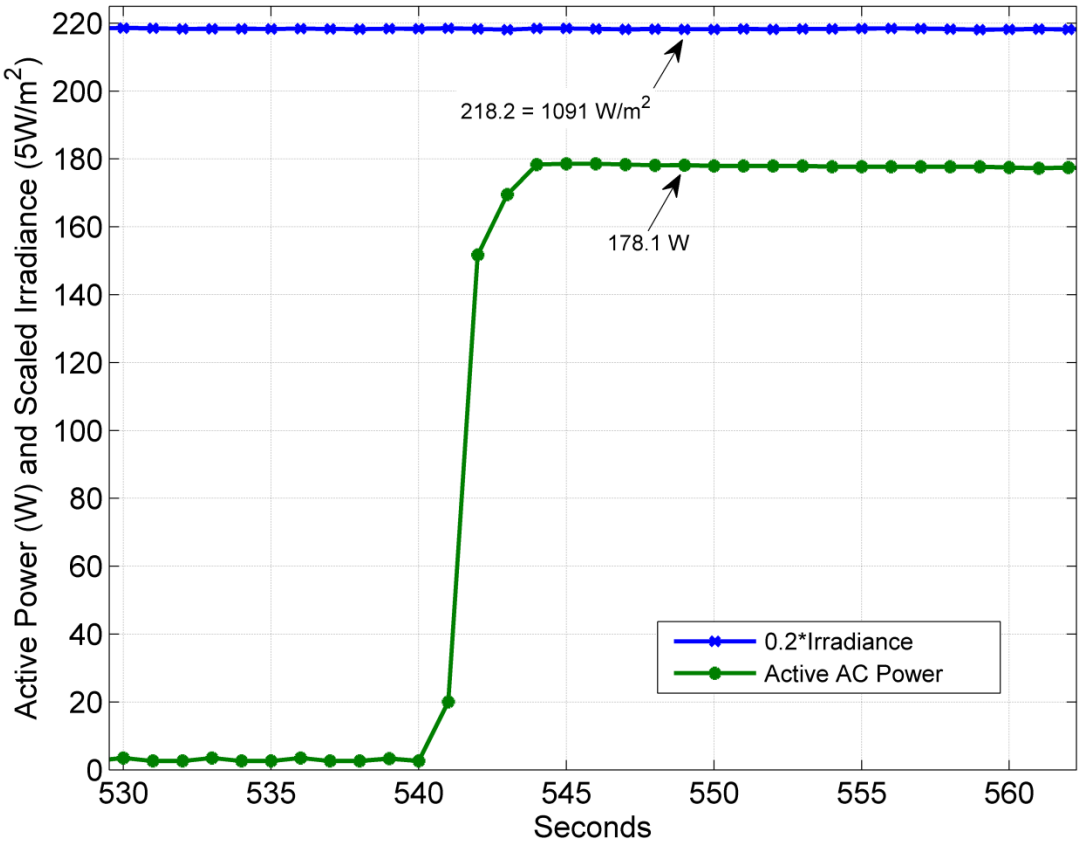

Figure 3: AC Module performance immediately before and after opaque cover removal during transient thermal test

After $E_{0,therm}$ and $P_{0,therm}$ have been selected, all of the measured AC power values are normalized to the thermal reference irradiance using equation 11.

$$P_{therm,adj} = P_{meas} \times \frac{E_{0,therm}}{E_{POA}} \quad \textbf{(11)}$$

The cell temperature must then be estimated (unless it is measured) from module temperature by a cell temperature model such as that presented in equation 7. A simple linear regression is then performed to find the linear function relating $P_{therm,adj}$ to the mean cell temperature in the form $f(T_c) = m_{th} \times T_c + b_{th}$ as shown in Figure 4. The AC module system's normalized response to cell temperature can then be easily found by equation 12.

$$\gamma_{ac} = \frac{m_{th}}{f(T_0)} = \frac{m_{th}}{m_{th} \times T_0 + b_{th}} \quad \textbf{(12)}$$

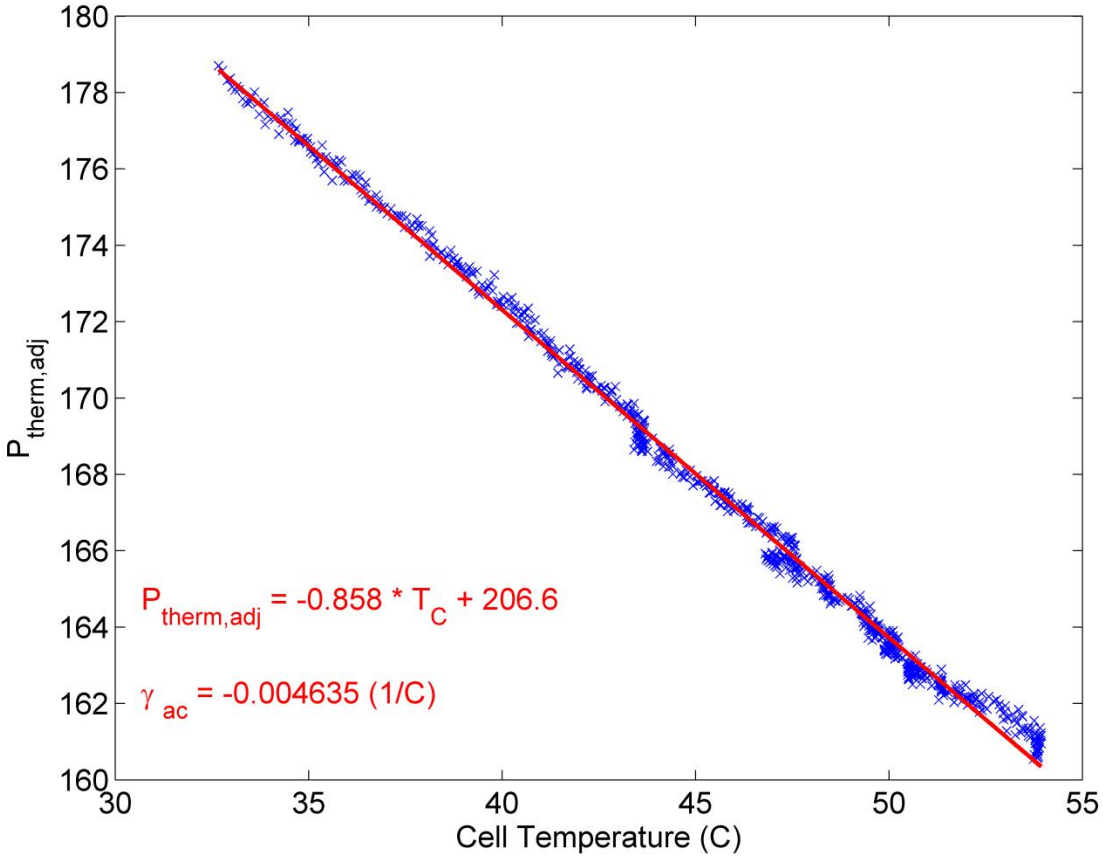

Figure 4: Regression of normalized power onto cell temperature and determination of γ_{ac}

4.2. Determining the Low Irradiance Power Level

In order to determine the low irradiance power level, simply record the active AC power consumed by the AC module under darkened conditions, as described in section 3.2.2. Figure 5 shows the active AC power measured from an AC module before sunrise. As shown, the AC module is steadily consuming 0.88 watts of active power prior to sunrise. Thus, P_{NT} is 0.88 and P_3 is -0.88.

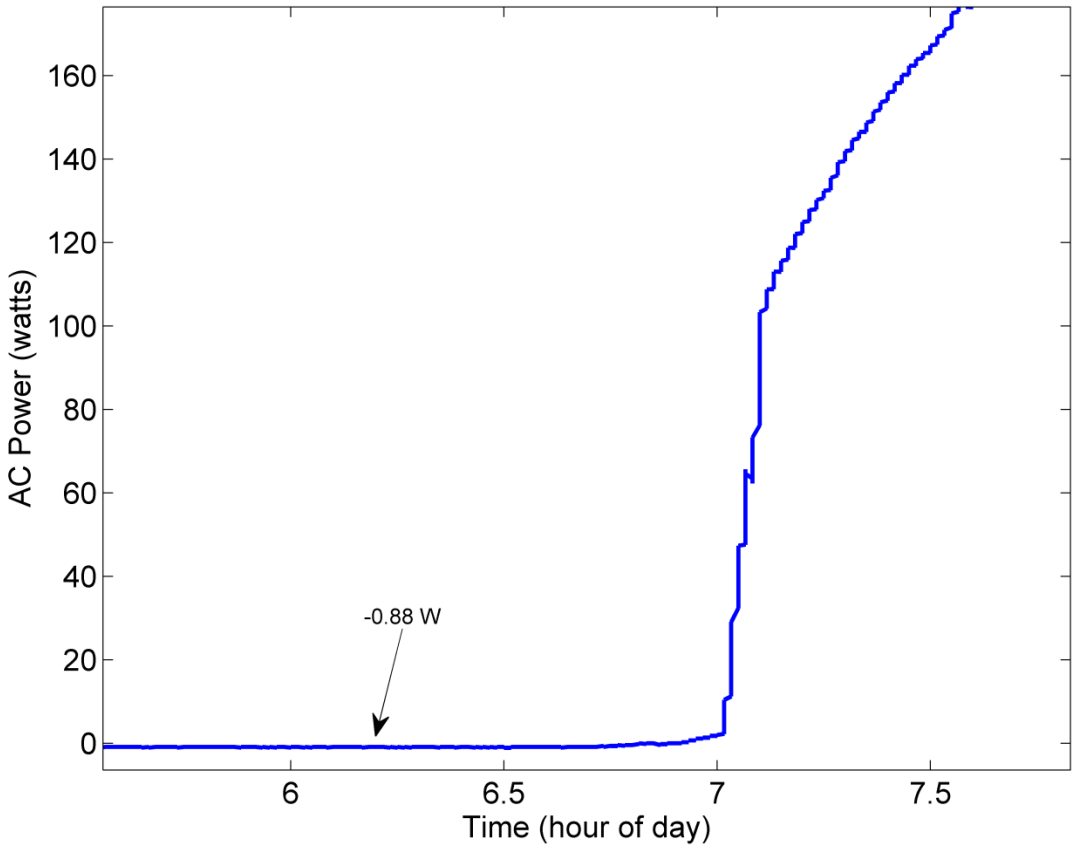

Figure 5: Determination of low-irradiance power level

4.3. Determining the Self-Limiting Power Level

Many microinverter manufacturers list the maximum rated output power of their inverters on their specification sheet. Presumably, the manufacturers of AC modules would also list the maximum rated values. If no empirical data are available to confirm the specification sheet value, for example if test conditions do not clearly show a self-limiting level, the specification sheet value may be used as the self-limiting power. However, we recommend determining the maximum AC power output empirically, as we have seen deviation between the specification sheet and measured maximum output power of 5% or more.

The self-limiting power level is determined by plotting the AC power as a function of POA irradiance. As shown in the inset of Figure 6, there seems to a clear maximum power which can be produced by the AC module. The main portion of Figure 6 shows that the maximum power level varies between 225 W and 229 W. In this case a constant value for the self-limiting power level, $P_{AC,max}$, is taken as the average power, 227 W. We note that the manufacturer specification sheet for the microinverter used in Figure 6 is 215 W, which underscores the fact that specification sheets may not accurately reflect the performance of a given model of microinverter or AC module.

As Figure 6 shows, it is possible that the maximum power level may actually vary and more accurate prediction of $P_{AC,max}$ may require a more involved expression than we use in equation 2.

While determining the maximum power level, it is important to also determine a power value below which the AC module is unlikely to be self-limiting (and thus is operating in the typical operation state at power P_1). This power level, denoted P_{clip}, is used in the following analyses to define test data gathered while the module was in the typical operation state. In this case, it is apparent that below 224 W the AC module is not self-limiting, thus P_{clip} is 224.

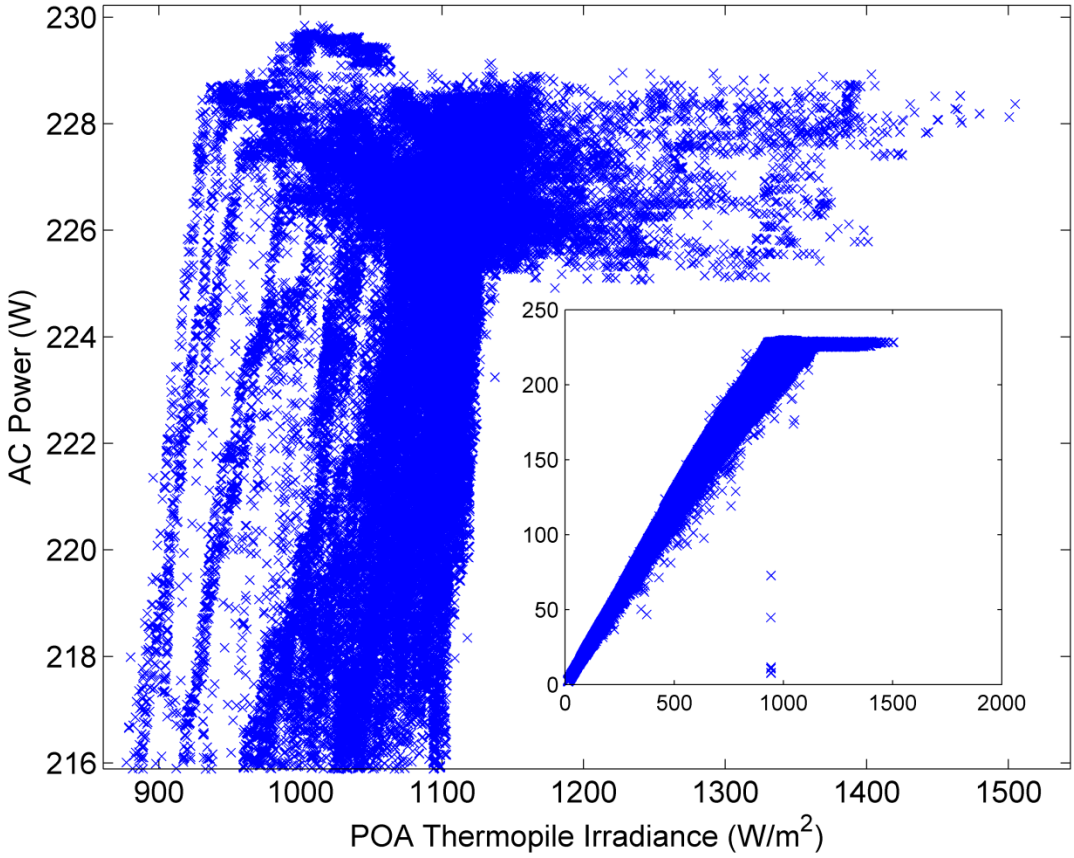

Figure 6: (Main) Power production at high POA irradiance. (Inset) Power production at all POA irradiance

4.4. Determining Reference Conditions

After examining the electrical performance test data to determine the power levels P_{NT} and $P_{AC,max}$ for the low irradiance and self-limiting states, respectively, the reference power, Pac_{ref}, reference airmass, AM_{ref}, and reference irradiance, E_{ref}, must be selected.

The reference conditions must represent clear-sky conditions, that is, data collected during times when there are no clouds within 20° of the sun and the local conditions are free from spectrum-altering conditions (haze, fog, smoke, etc.), and when the AC module system is not self-limiting. The analyst should plot clear-sky data of POA irradiance as a function of absolute airmass, data with output power greater than the previously determined P_{clip} should be somehow denoted differently than the data with output power less than P_{clip}, as shown in Figure 7. The analyst must select an irradiance and airmass range in which the inverter was tested, and self-limiting was unlikely. Ideally the irradiance should be near 1000 W/m^2 and absolute airmass should be near 1.5. However, depending on the AC module and the test location, the ideal conditions may not be present in the electrical performance data set. In Figure 7, it can be seen that there were no data points collected near 1000 W/m^2 and AM_a equal to 1.5. It can also be seen that for clear-sky conditions with airmass less than 1.5, the test site usually had such high POA irradiance that the AC module was self-limiting (clipping), thus AMa_{ref} should not be selected to be below 1.5. We see that at a POA irradiance of 1000 W/m^2, most of the data do not show the module to be self-limiting, and this irradiance generally occurs near absolute airmass 1.7. Therefore, for this module, E_{ref} is selected to be 1000 W/m^2 and AMa_{ref} is selected to be 1.7, as shown in Figure 8.

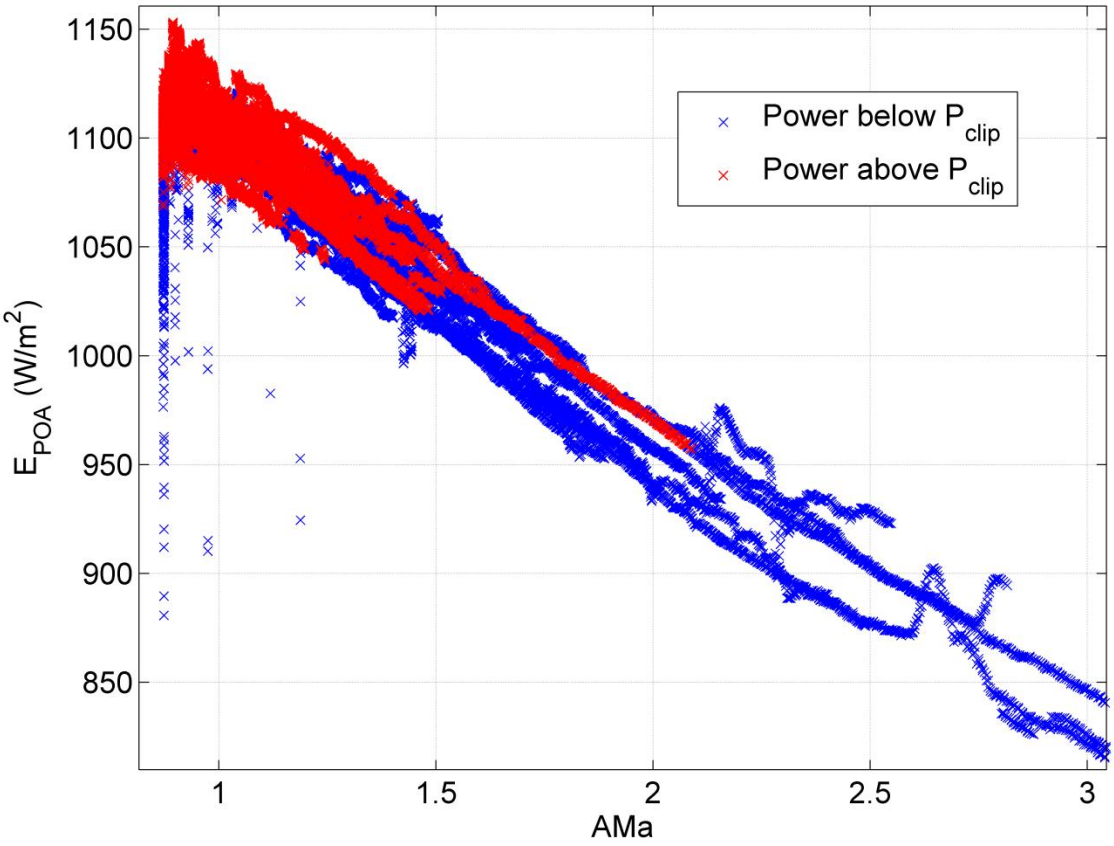

Figure 7: Plot of POA irradiance as a function of airmass with clipping data denoted

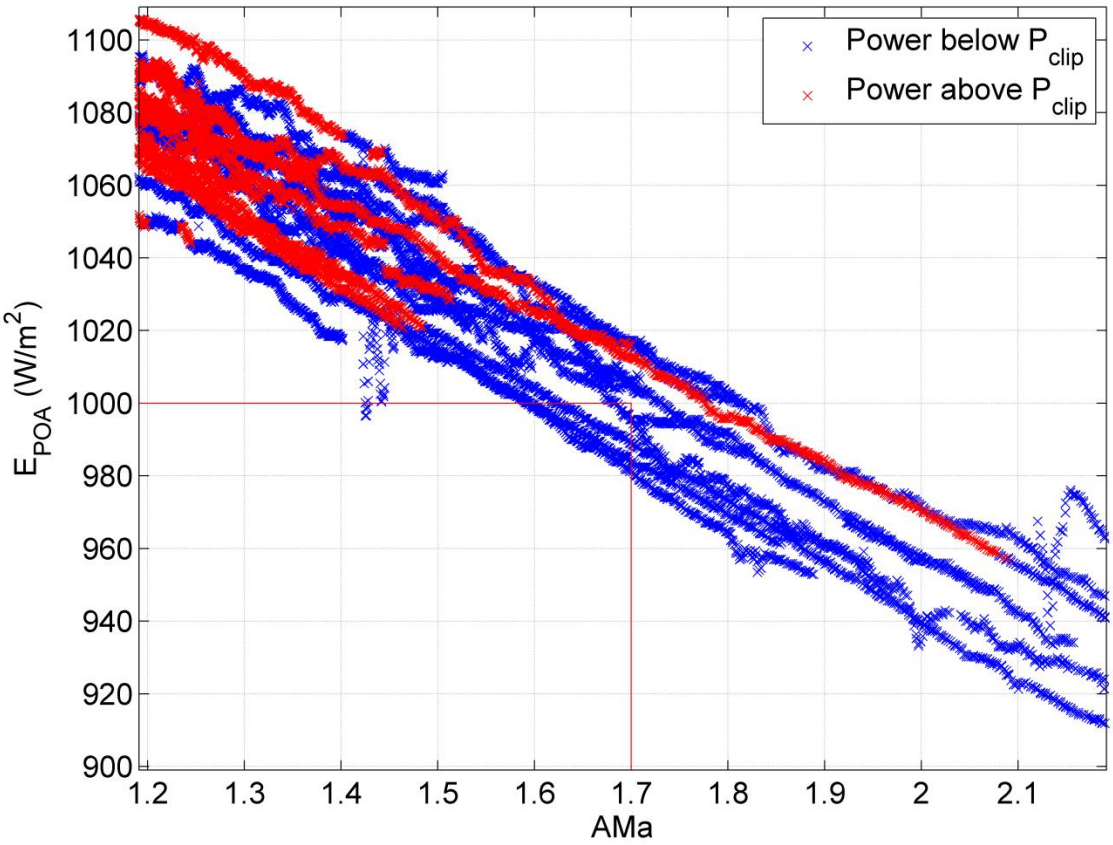

Figure 8: Reference irradiance and airmass selected

After determination of the reference irradiance and airmass, the reference power must be selected such that the AC module produces the reference power when operating at the reference irradiance, reference airmass, and reference cell temperature. As it is unlikely that all three of the reference conditions were experienced during the electrical performance testing, it is necessary to tightly bin the data and correct for deviation from reference conditions.

We have binned the data within 0.05 airmass units around AMa_{ref}, and plotted the temperature adjusted power Pac_{Tc-T0} (equation 13) as a function of E_{POA}, then performed a linear regression and evaluated the regression at $E_{POA} = E_{ref}$. Thus, for the data shown in Figure 9, Pac_{ref} is 239.1 W. The fact that Pac_{ref} is greater than $P_{AC,max}$ does not matter. This simply indicates that at the reference irradiance, airmass, and temperature conditions the AC module is predicted to produce $P_{AC,max}$.

$$Pac_{Tc-T0} = \frac{Pac}{1+\gamma_{ac}(T_C - T_0)} \quad \textbf{(13)}$$

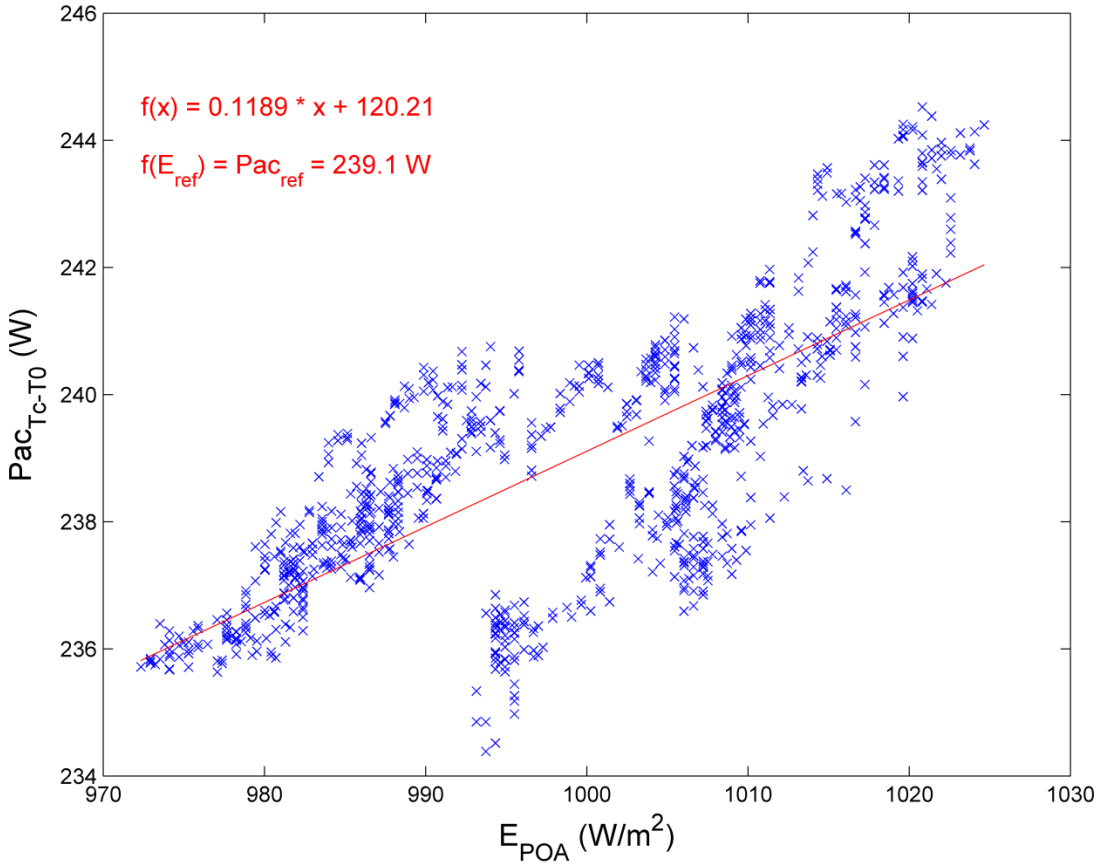

Figure 9: Temperature-adjusted power as a function of airmass with regression.

4.5. Determining the Effect of Solar Spectrum

To determine the effect of solar spectrum on power output of the AC module, the data must contain only clear-sky data and when the produced power is less than P_{clip} and the solar AOI is 0. These restrictions are necessary to observe the effect of solar spectrum on module power separately from other effects. These restrictions also limit the irradiance range in the data, typically between 500 and 1200 W/m^2. At these irradiance conditions, the relationship between irradiance and output power is approximately linear, thus for these data, we may simplify equation 4 by assuming C_0 equals 1 and C_1 equals 0. Empirical values for C_0 and C_1 are determined later over a larger range of irradiance. If a third order polynomial form of f_1 as given in equation 8 is used to model the variation in power with changing airmass, then equation 4 can be rewritten as equation 14, or in matrix form as a system of equations as in equation 15.

$$\frac{Pac}{Pac_{ref}\times[1+\gamma_{ac}(T_c-T_0)]} - \frac{E_{POA}}{E_{ref}} = \frac{E_{POA}}{E_{ref}} \times A_1 \times \left(AMa - AMa_{ref}\right) + \frac{E_{POA}}{E_{ref}} \times A_2 \times \left(AMa - AMa_{ref}\right)^2 + \frac{E_{POA}}{E_{ref}} \times A_3 \times \left(AMa - AMa_{ref}\right)^3 \quad \textbf{(14)}$$

$$\left[\frac{E_{POA}}{E_{ref}} \times \left(AMa - AMa_{ref}\right) \quad \frac{E_{POA}}{E_{ref}} \times \left(AMa - AMa_{ref}\right)^2 \quad \frac{E_{POA}}{E_{ref}} \times \left(AMa - AMa_{ref}\right)^3\right] \times \begin{bmatrix} A_1 \\ A_2 \\ A_3 \end{bmatrix} = \left[\frac{Pac}{Pac_{ref} \times [1+\gamma_{ac}(T_c - T_0)]} - \frac{E_{POA}}{E_{ref}}\right] \quad \textbf{(15)}$$

The unknowns A_1, A_2, and A_3 are determined by finding the least-squares solution to the system of equations presented in equation 15.

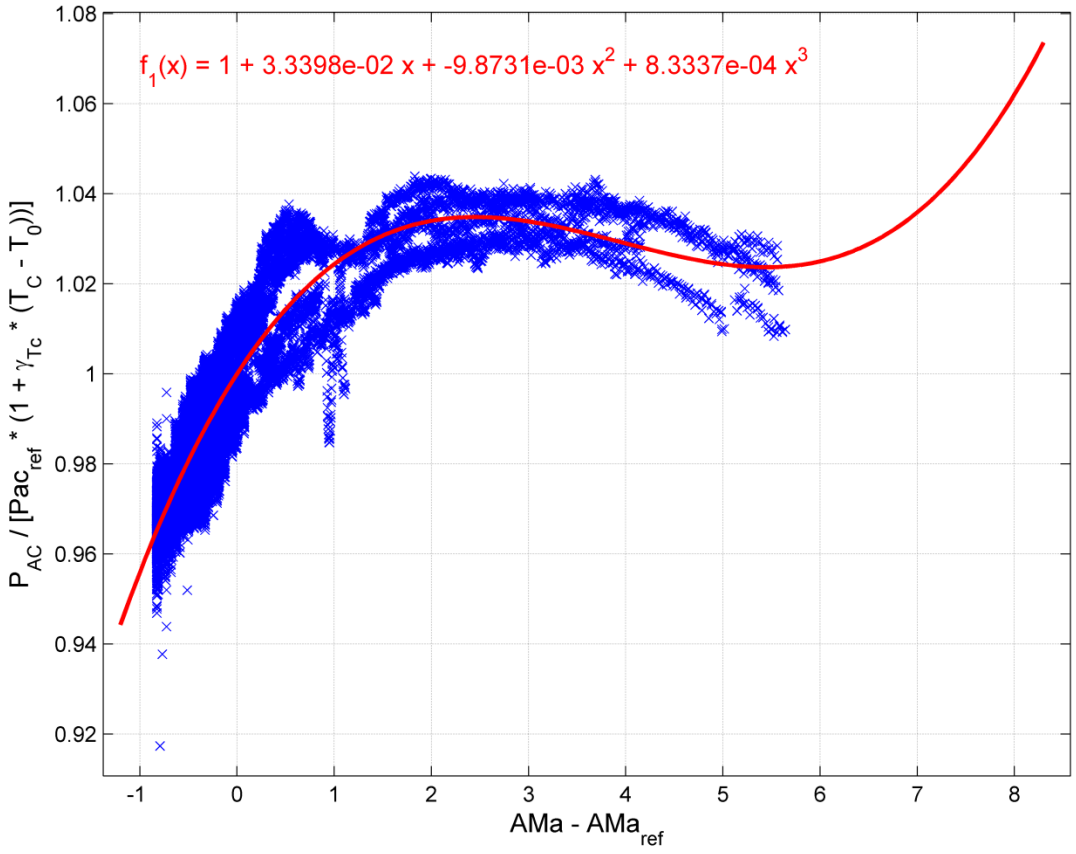

Figure 10: Normalized AC power variation with airmass

As Figure 10 shows, the f_1 function fits the data well for absolute airmass values between -0.7 and +5.5 around the reference airmass. When the airmass is more than 5.5 above the reference airmass, there is little data, and the polynomial quickly trends upward to unrealistic values. Thus, we recommend that modelers examine the possible values of f_1 and limit the maximum and minimum value of f_1 to values which are realistic.

4.6. Determining the Irradiance Relationship

After we have determined the reference values and airmass to power relationship, f_1, the relationship between irradiance and power may be established by using all electrical performance

data where the AC module was producing power less than P_{clip} (i.e. data during clear-sky and cloudy-sky conditions should be used as long as the AC module was not self-limiting) and operating with POA irradiance greater than 10 W/m^2.

Once the parameters of $f_1(AMa - AMa_{ref})$ are known, it is possible to rewrite equation 4 as equation 16, which can be written in matrix form as a system of equations such as shown in equation 17.

$$\frac{Pac}{Pac_{ref} \times [1+\gamma_{ac}(T_c - T_0)] \times f_1(AMa - AMa_{ref})} = C_0 \times \frac{E_{POA}}{E_{ref}} + C_1 \times \ln\left(\frac{E_{POA}}{E_{ref}}\right) \quad \textbf{(16)}$$

$$\left[\frac{E_{POA}}{E_{ref}} \quad \ln\left(\frac{E_{POA}}{E_{ref}}\right)\right] \times \begin{bmatrix} C_0 \\ C_1 \end{bmatrix} = \left[\frac{Pac}{Pac_{ref} \times [1+\gamma_{ac}(T_c - T_0)] \times f_1(AMa - AMa_{ref})}\right] \quad \textbf{(17)}$$

The values of C_0 and C_1, are then determined by finding the least-squares solution to the system of equations presented in equation 17. A sample of the resulting model along with the input data is shown in Figure 11.

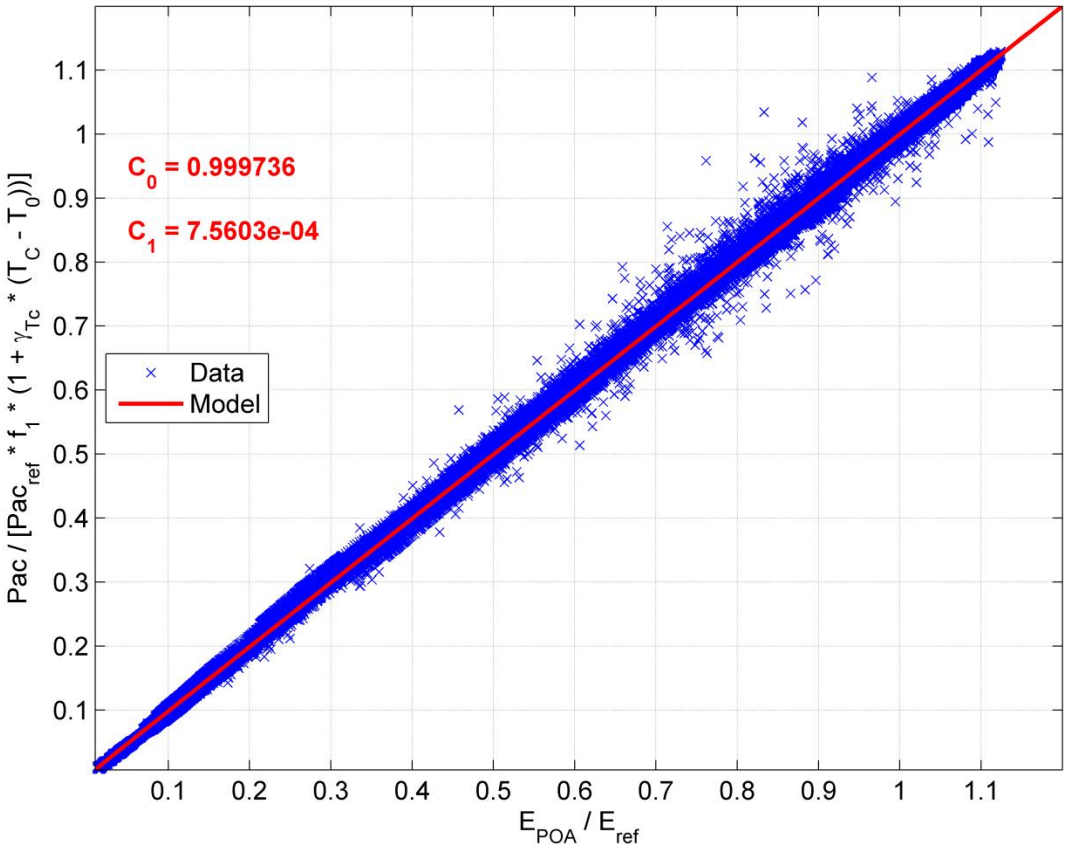

Figure 11: Fit for C_0 and C_1 with test data

4.7. Determine Module Back Temperature from Irradiance, Wind Speed, and Ambient Temperature

If the simple model is used for determination of average module backside temperature given ambient temperature, irradiance, and wind speed (equation 6), the coefficients a and b must be determined from the electrical performance test data. This module temperature model assumes that the module is in near thermal equilibrium, thus only clear-sky data periods may be used to determine a and b since cloudy conditions may present temperature transients due to intermittent cloud cover. Furthermore, only data where the AC module is producing power less than P_{clip} should be used, as self-limiting may generate additional thermal energy within the module.

The coefficients a and b are found by writing equation 6 as equation 18, then performing a least squares fitting of exponential data as in [27]. The equations to find the coefficients a and b which minimize the least square errors are equation 19 and 20. The resulting data and model fit are shown in Figure 12.

$$\frac{(T_m - T_a)}{E} = e^{a+b\times WS} \quad \textbf{(18)}$$

$$a = \ln\left[\frac{\sum_{i=1}^{n}(x_i^2 y_i)\sum_{i=1}^{n}(y_i \ln y_i) - \sum_{i=1}^{n}(x_i y_i)\sum_{i=1}^{n}(x_i y_i \ln y_i)}{\sum_{i=1}^{n}(y_i)\sum_{i=1}^{n}(x_i^2 y_i) - \left(\sum_{i=1}^{n}(x_i y_i)\right)^2}\right] \quad \textbf{(19)}$$

$$b = \frac{\sum_{i=1}^{n}(y_i)\sum_{i=1}^{n}(x_i y_i \ln y_i) - \sum_{i=1}^{n}(x_i y_i)\sum_{i=1}^{n}(y_i \ln y_i)}{\sum_{i=1}^{n}(y_i)\sum_{i=1}^{n}(x_i^2 y_i) - \left(\sum_{i=1}^{n}(x_i y_i)\right)^2} \quad \textbf{(20)}$$

where x is the wind speed (WS) and y is $\frac{(T_m - T_a)}{E}$.

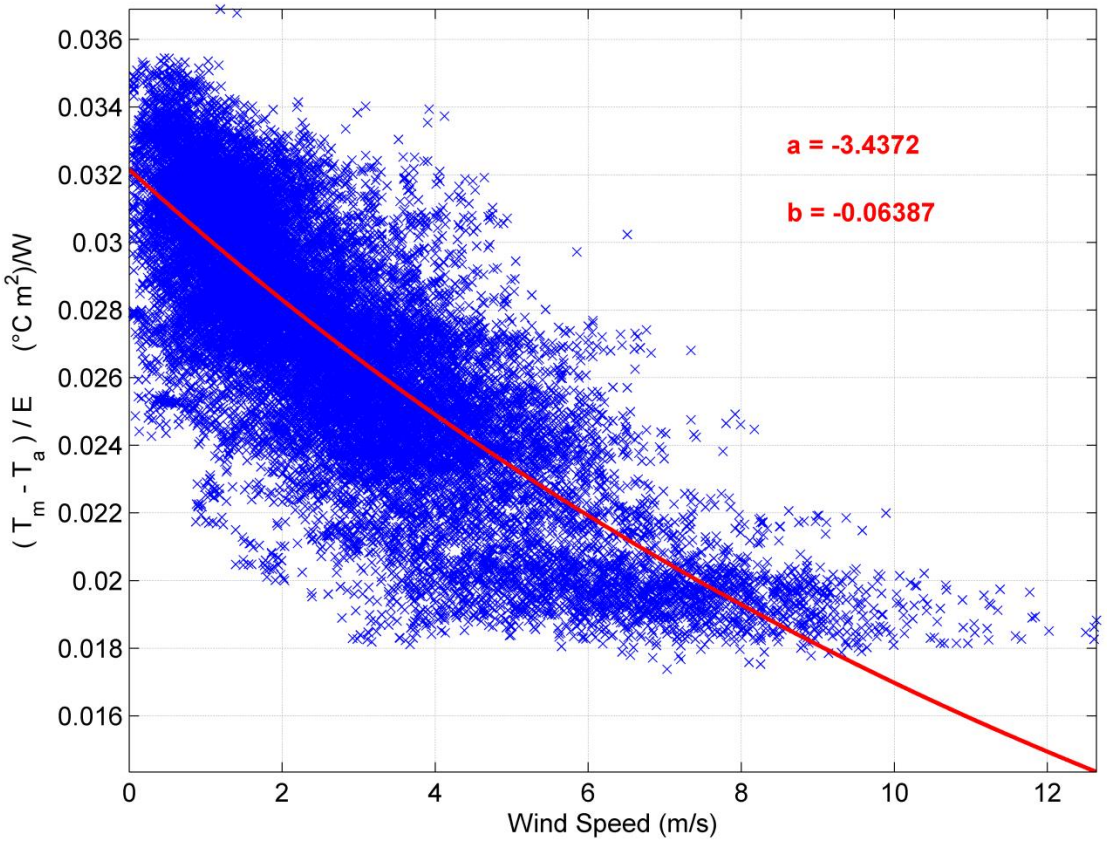

Figure 12: Relationship between average module temperature and wind speed, ambient temperature, and irradiance

4.8. Determine Incident Angle Response

In order to account for nonzero solar incident angles and losses of beam irradiance due to reflections off the module's surface, we introduce a reflection loss function $f_2(\theta)$ as shown in equation 10. The necessary data for determining f_2 is obtained through the AOI test.

To find f_2, we must solve explicitly for f_2 after substituting for E_{POA} from equation 4 into equation 10 as shown in equation 18.

$$Pac = Pac_{ref} \times f_1(AMa - AMa_{ref}) \times \left[C_0 \times \frac{E_b \times f_2(\theta) + E_{diff}}{E_{ref}} + C_1 \times \ln\left(\frac{E_b \times f_2(\theta) + E_{diff}}{E_{ref}}\right)\right] \times [1 + \gamma_{ac}(T_c - T_0)] \quad \textbf{(18)}$$

However, rather than using the typical value of Pac_{ref} to determine f_2, we establish a separate reference power, Pac_r, which is specific to the time period during the incident angle test. Pac_r is determined using the incident angle test data obtained while $\theta = 0$ at the beginning of the incident angle test as in equation 19. It is important to generate Pac_r rather than relying on

Pac_{ref} in order to more precisely normalize the power data obtained during the incident angle test.

$$Pac_r = mean\left\{\frac{Pac_{A0}}{f_1(AMa_{A0}-AMa_{ref})\times\left[C_0\times\frac{E_{POA,A0}}{E_{ref}}+C_1\times\ln\left(\frac{E_{POA,A0}}{E_{ref}}\right)\right]\times[1+\gamma_{ac}(T_{c,A0}-T_0)]}\right\} \quad (19)$$

where:

Pac_r is a reference power established with data obtained when $\theta = 0$ and less than 10 minutes before the incident angle test and the module has a stable temperature

Pac_{A0} is the AC power values measured less than 10 minutes before the incident angle test while $\theta = 0$

AMa_{A0} is the absolute airmass at which each Pac_{A0} data point was measured

$E_{POA,A0}$ is the plane of array irradiance at which each Pac_{A0} data point was measured

$T_{c,A0}$ is the cell temperature of the AC module at which each Pac_{A0} data point was measured

For all data points during the incident angle test, we generate a normalized power by translating all measured power data to reference conditions and dividing by Pac_r. By then solving this normalized power as an explicit function of f_2 we establish that f_2 describes changes in the normalized power due to changes solar incident angle. An intermediate step in this algebra is shown in equation 20 for clarity.

$$\frac{Pac}{Pac_r\times f_1(AMa-AMa_{ref})\times[1+\gamma_{ac}(T_c-T_0)]} = C_0\times\frac{E_b\times f_2(\theta)+E_{diff}}{E_{ref}} + C_1\times\ln\left(\frac{E_b\times f_2(\theta)+E_{diff}}{E_{ref}}\right) \quad (20)$$

For brevity in the subsequent equations, we make the following substitution:

$$v = \frac{Pac}{Pac_r\times f_1(AMa-AMa_{ref})\times[1+\gamma_{ac}(T_c-T_0)]} \quad (21)$$

Equation 22 is the result of solving equation 20 explicitly for $f_2(\theta)$.

$$f_2(\theta) = \left[\frac{C_1\times W\left(\frac{C_0}{C_1}\times e^{\frac{v}{C_1}}\right)\times E_{ref}}{C_0} - E_{diff}\right]\Big/ E_b \quad (22)$$

Where $W(x)$ is the Lambert W function (an excellent explanation of the Lambert W function can be found at [28]). To date, all of Sandia's analyses have resulted in $\frac{C_0}{C_1}$ values greater than 0, and thus the upper part of the principal branch of the Lambert W function is used.

From equation 22, it is possible to determine any desired functional form of f_2. However, we have chosen to use the functional form of f_2 according to [14], thus we must find the value of a_r which provides the best fit to the data. Determination of a_r is possible through the use of an optimization algorithm, seeking an a_r value which minimizes the mean squared error between equation 22 and equation 23.

$$f_2(\theta) = \left(1 - e^{\frac{-\cos(\theta)}{a_r}}\right) \Big/ \left(1 - e^{\frac{-1}{a_r}}\right) \quad \textbf{(23)}$$

Figure 13 shows sample data and analysis results for determining the response of an AC module to incident angle.

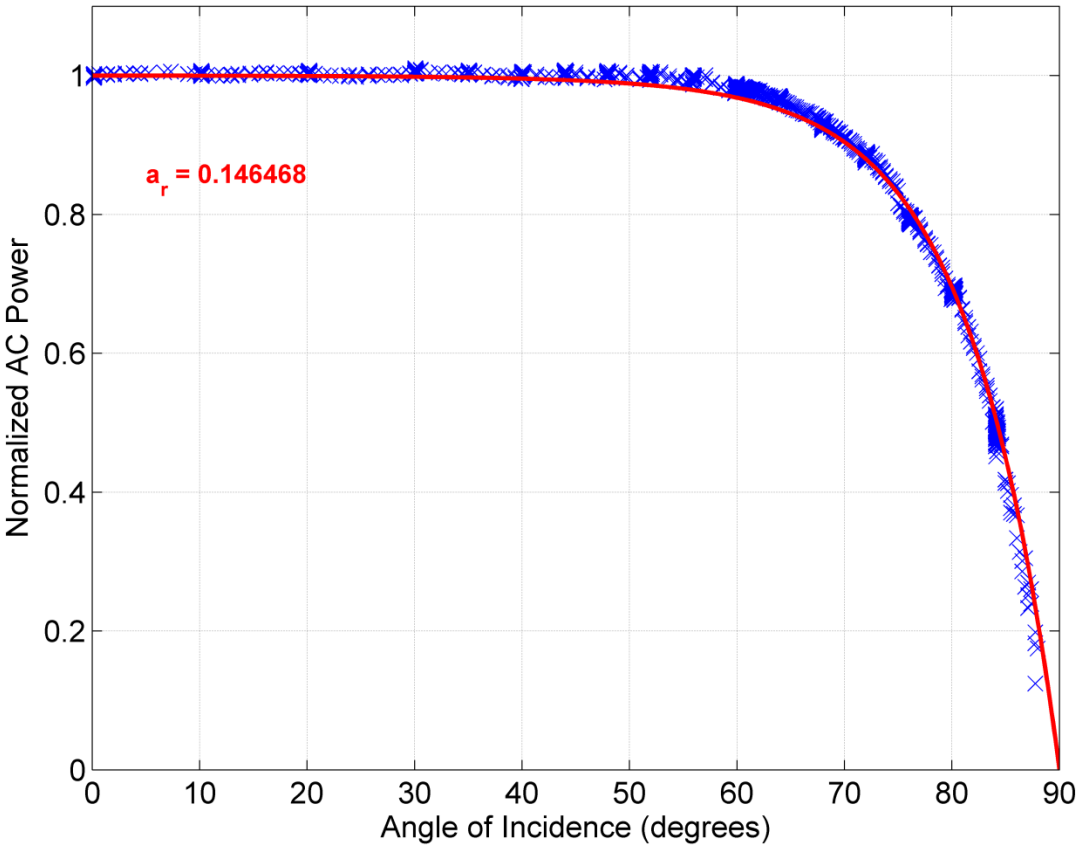

Figure 13: Sample data and results from determining an AC module's response to AOI

5. MODEL ACCURACY AND VALIDATION

The proposed model is evaluated here in two ways, first by examining the ability of the model to reproduce the test data which were used to generate the model parameters (the electrical performance test data), second by examining the accuracy of the model in predicting the power of an AC module during common operations and using data which were not used to generate model parameters. The first evaluation is not validation of the model, but rather serves to show how well the model form can describe the AC module under ideal conditions. The second evaluation is a validation of the entire model, demonstrating how well the model predicts AC module performance under real-world conditions including variations in incident angle.

The model validations performed to date are limited to the operating conditions in Albuquerque, New Mexico. More rigorous validation of the model should evaluate if the model parameters are applicable across multiple types of environmental regions. For example, model parameters should be developed at one location and the developed model should be operated and evaluated against actual performance data gathered at multiple locations.

5.1. Accuracy of the Model in Reproducing the Electrical Performance Test Data

In order to develop the AC module model, Sandia tested four different AC modules with varying types of PV modules and microinverters. Model parameters were developed for each module and the resulting model was compared against the measured data in the electrical performance data set. This comparison simply shows how well the model describes the performance data used to generate the model parameters.

The difference between the modeled power and the measured power is expressed in Table 1 as both the mean bias error (MBE, positive values indicate the model over-predicted the power) and the root mean square error (RMSE).

Table 1. Model Error Statistics for Electrical Performance Test Data

	MBE (watts)	MBE (% of Pac_{ref})	RMSE (watts)	RMSE (% of Pac_{ref})
AC Module 1	0.1213	0.0507	2.2287	0.9321
AC Module 2	0.0739	0.0419	2.1578	1.2230
AC Module 3	0.0572	0.0228	2.5448	1.0142
AC Module 4	0.1075	0.0421	2.5000	0.9801

Figures 14 through 17 show histograms of the model residuals (modeled power – measured power) as a percentage of Pac_{ref} for each AC module (daytime only) during the electrical performance test. For all of the AC modules, the errors are generally distributed with a mean value near 0, and the majority of the errors are less than 2% of Pac_{ref}.

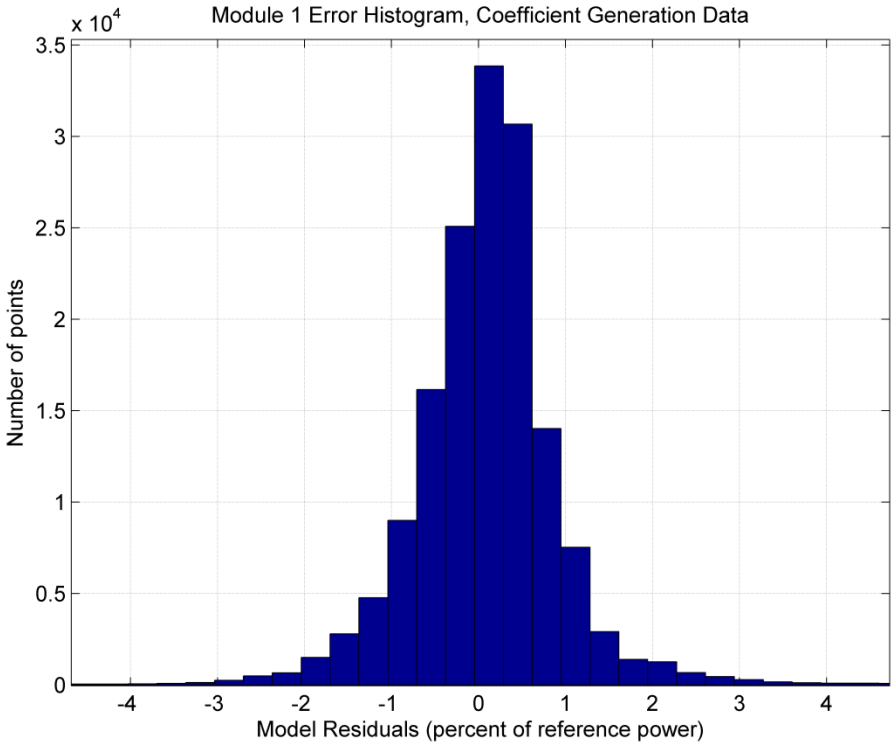

Figure 14: Model residual histogram for Module 1 with electrical performance test data

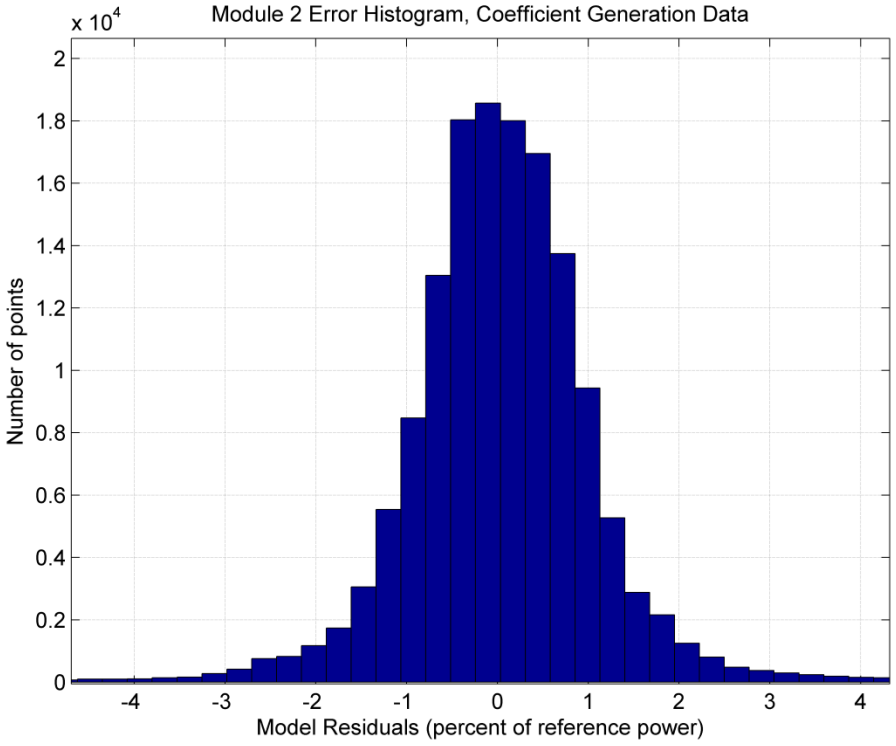

Figure 15: Model residual histogram for Module 2 with electrical performance test data

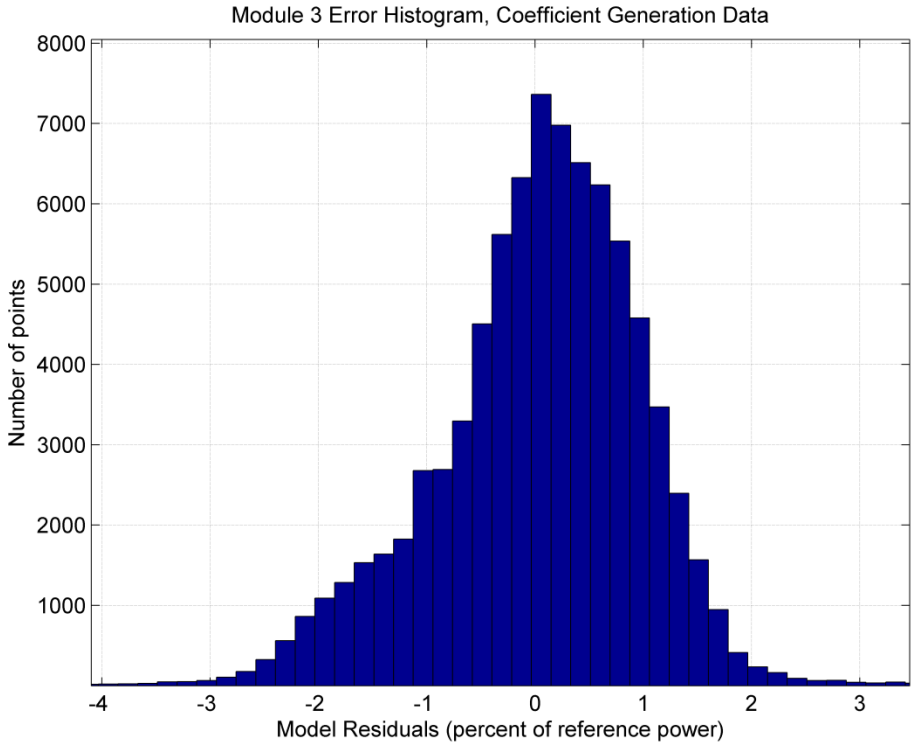

Figure 16: Model residual histogram for Module 3 with electrical performance test data

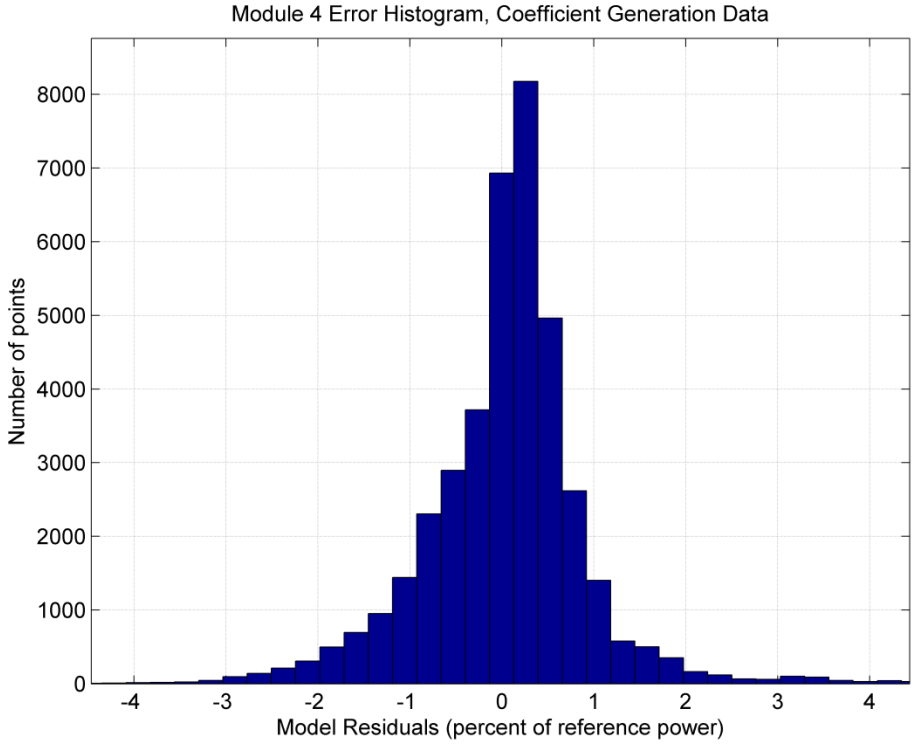

Figure 17: Model residual histogram for Module 4 with electrical performance test data

5.2. Validation of the Model on Fixed-Tilt AC Modules

In order to validate the model, several of the AC modules were mounted at a fixed-tilt orientation and were monitored. The previously generated model parameters were used to predict the power output of the modules, and predictions were compared with the measured power. The module back-surface temperature was measured by thermocouples and cell temperature was estimated using equation 7 (thus a temperature model relating ambient temperature to module temperature such as in equation 6 was not used). The DNI and plane of array irradiance were measured to calculate E_{POA}.

The following validation results are from Module 3, which was mounted facing south at a 35 degree tilt from horizontal for 9 days. The days were mostly sunny, with some cloudy or partly cloudy periods.

The modeled power and measured power for a clear day and a partly cloudy day are shown in Figures 18 and 19, respectively. Note on both days that there is significant difference between measured and modeled power at the very end of the day, near sunset. These differences are due to shading of the AC module while the irradiance instruments were unshaded, and do not indicate a defect in the model. These data have been removed in all subsequent analyses and plots. The steep rise in power in the morning is due to the abrupt rise of the sun over the mountains which lie east of the test location.

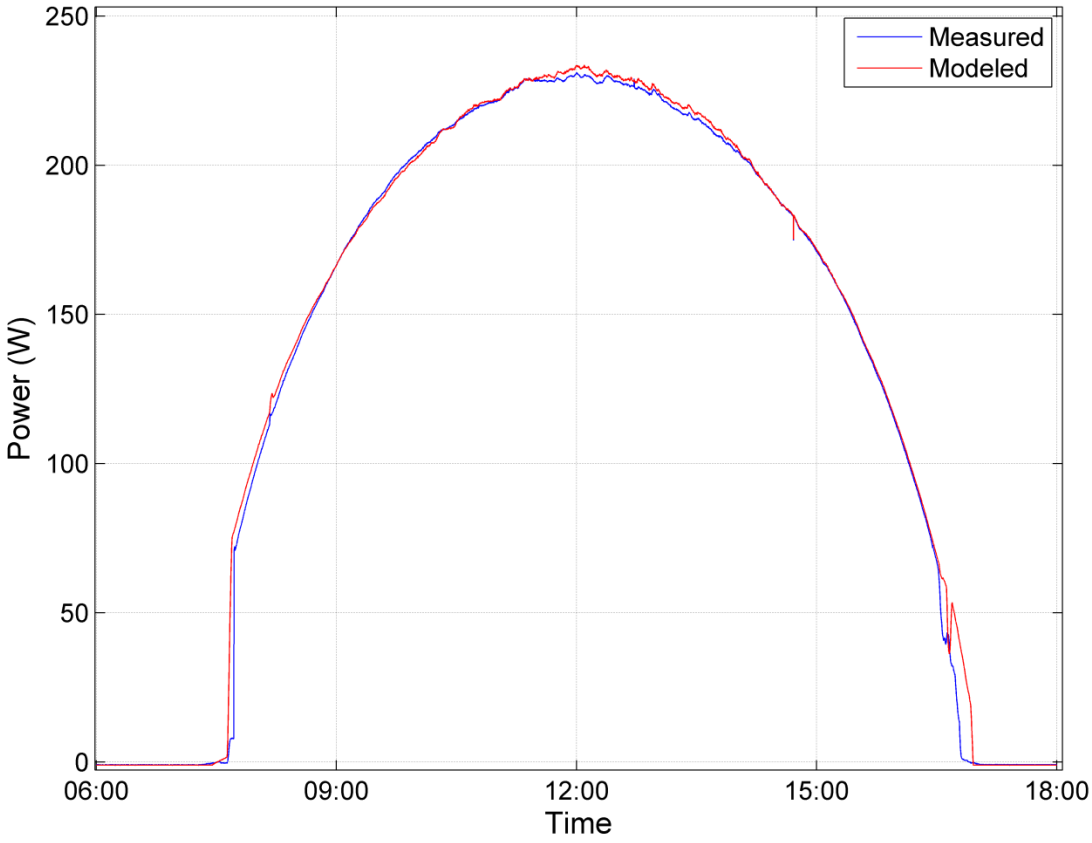

Figure 18: Measured and modeled power from a fixed-tilt AC module on a cool, calm, sunny day

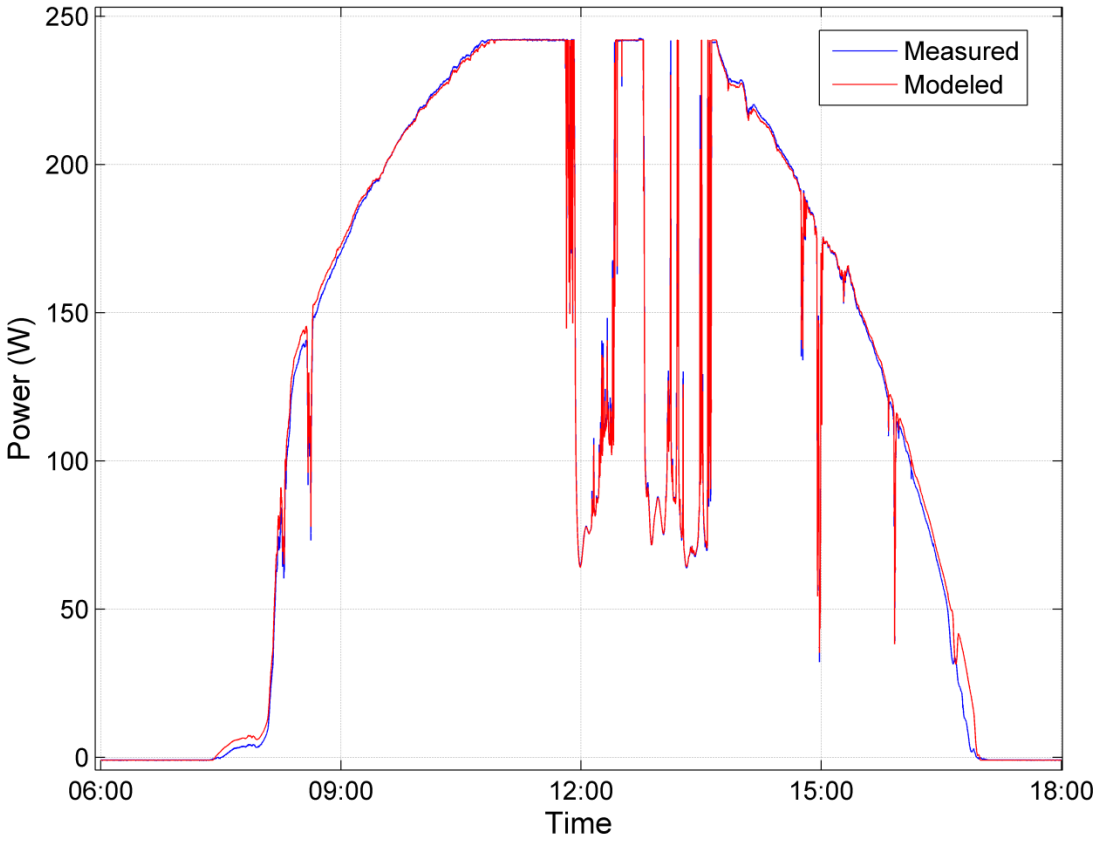

Figure 19: Measured and modeled power from a fixed-tilt AC module on a cold, breezy, partly cloudy day

When plotting the modeled power as a function of measured power, as in Figure 20, it is easy to see that the model is generally performing better at high power levels (high irradiance), and that it tends to over-predict the power, especially at low and medium power levels.

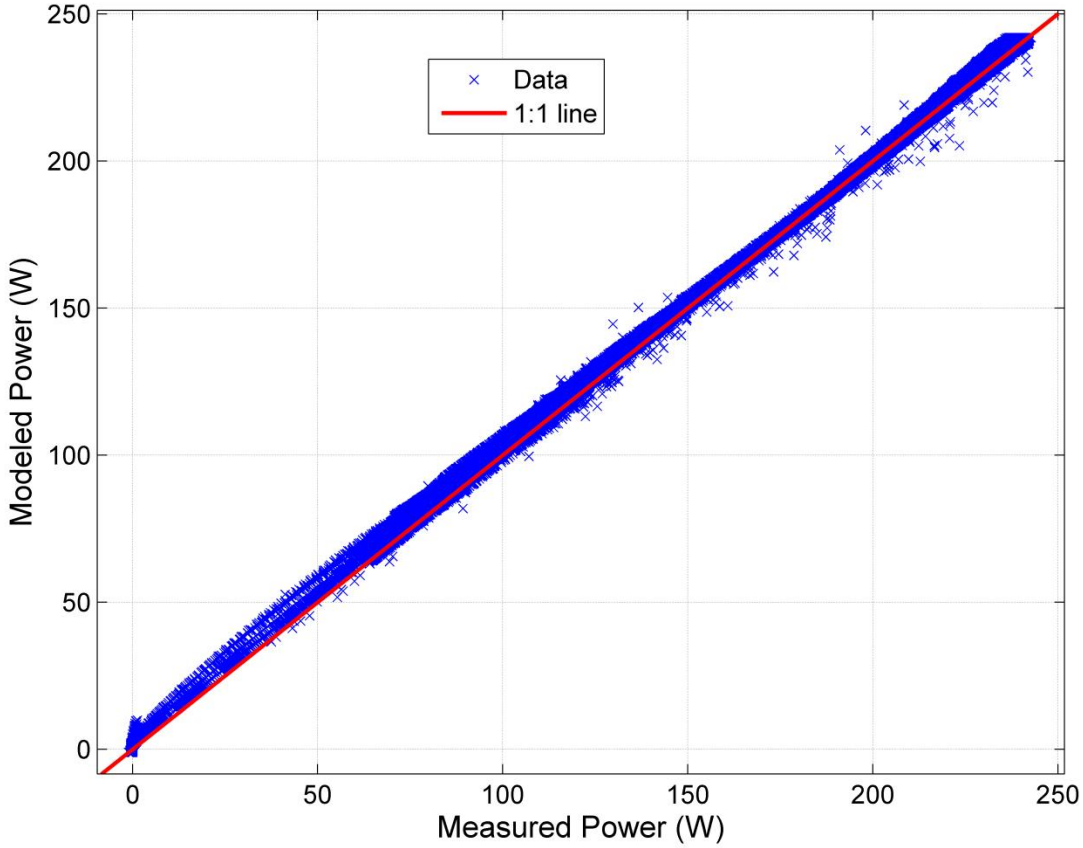

Figure 20: Modeled power as a function of measured power over 9 days for a fixed-tilt AC module

A histogram of model errors as a percentage of Pac_{ref}, as shown in Figure 21, also shows that the model is generally over-predicting the output of the AC module. The data in Figure 21 are for the day time only (sun elevation greater than 6°). A histogram of all data (i.e., including night-time periods) is unhelpful since the model is extremely good at predicting power during the night. The error distribution is clearly much more positively biased than the error distribution shown in Figure 16, but most errors are in the range of -0.5% to +2.5% of Pac_{ref}.

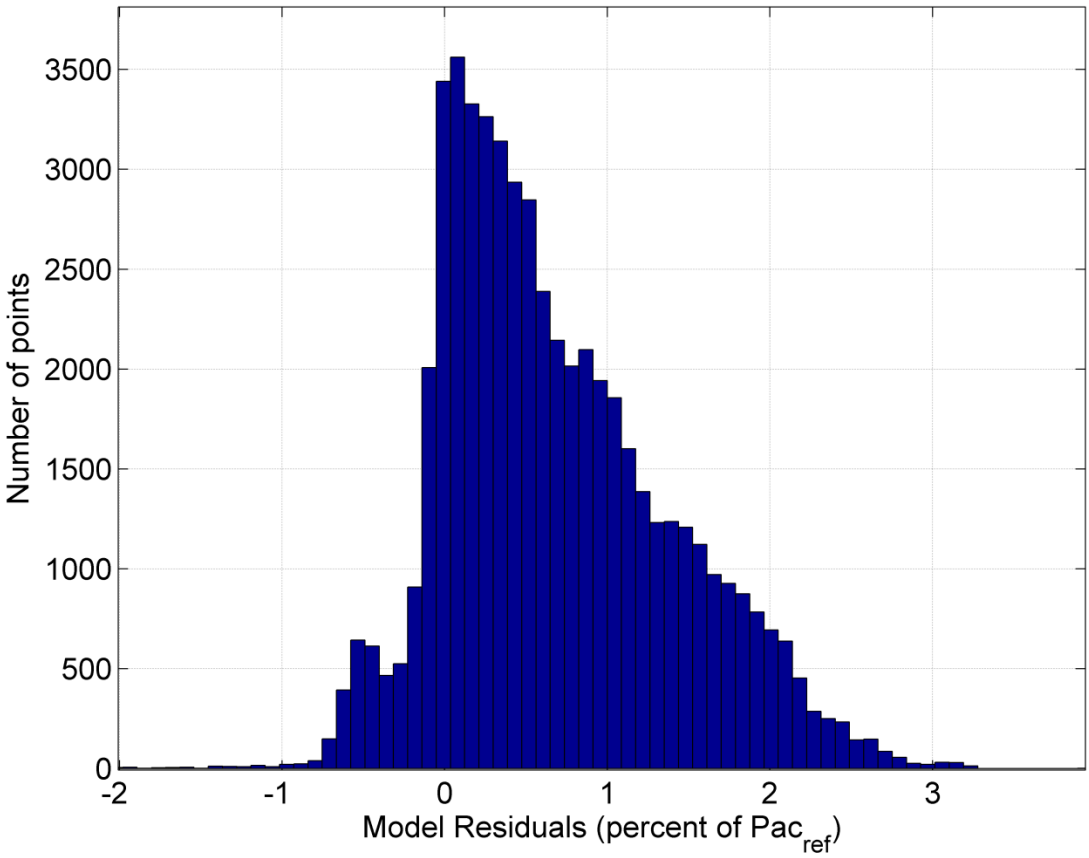

Figure 21: Histogram of model power residuals over 9 days for a fixed-tilt AC module, daytime data only

The model residuals for this module are positively biased when the module is operated in a fixed-tilt orientation whereas the residuals were unbiased while the module operated with 0° solar AOI (see Figure 16). This shift is likely due to inaccuracies in the f_2 function, or correlations in functions which were assumed to be independent (e.g. the transmission of the front surface changes with spectrum).

Over the course of 9 days, the AC module generated 14.377 kWh of energy and the model predicted the module would produce 14.584 kWh.

Table 2 describes the performance of the model according to several common metrics. Note that the periods where the module was shaded in the afternoon have been removed (approximately 20 minutes per day) in order to reflect the model's ability to predict power under normal circumstances.

Table 2. Model Error Statistics Module 3, Fixed Tilt

	MBE (watts)	MBE (% of Pac_{ref})	RMSE (watts)	RMSE (% of Pac_{ref})
Daytime only, shading removed	1.700	0.6776	2.484	0.9903
Day and night, shading removed	0.648	0.2584	1.688	0.6729

6. CONCLUSIONS

Sandia National Laboratories has developed an empirical performance model for describing the performance of PV modules with integrated microinverters, also known as AC modules, as a function of various environmental conditions. The model seeks to predict the active AC power which is produced by an AC module at a given temperature, under a given irradiance and absolute airmass condition The coefficients or parameters which describe the AC module performance are somewhat similar to the coefficients found in performance models for standalone PV modules, however, several reference conditions must be specified since all AC modules may not be in the typical operating state (i.e. may be self-limiting) at the conventional reference conditions of 1000 W/m^2, ASTM G173 spectrum, and 25 °C cell temperature. The performance model includes descriptions of the performance when the AC module is self-limiting or "clipping" its power, as well as describing performance when the AC module is under extremely low-irradiance such as at night. The addition of limiting conditions for low-irradiance and self-limiting will improve the energy yield predictions over long periods of time.

The model for the typical operating state is formed as a series of multipliers to a reference power. The multipliers are a set of normalized sub-models which describe the normalized performance changes of the AC module as a function of a particular variable (or variables). Thus the model is flexible, since new sub-models may be introduced which better describe the performance of the AC module as a function of the particular variable. We have proposed a series of recommended sub-models for use within the model.

We have also described a series of outdoor tests which may be performed in order to generate the necessary performance coefficients for use in the model. These tests attempt to hold constant some environmental conditions surrounding the AC module while allowing specific conditions to vary.

Once the series of tests have been conducted, we have shown how to transform the test data into the model coefficients. Where we have suggested specific sub-models (e.g. incident angle modifier models, cell temperature models, airmass models) we have shown the process to obtain model coefficients for those sub-models from test data.

Lastly, we have shown that for the AC modules which we tested, the model is capable of predicting the power of an AC module in a fixed-tilt orientation with a root mean square error of 1 %. The model successfully predicted the energy of an AC module system over the course of 9 days to within 1.4 % of the actual produced energy.

The AC module performance model presented here may be used to characterize and subsequently predict the AC energy output of system of AC modules. The model may also be used to compare the performance of two different AC modules. We further propose that the model may be useful in establishing a performance standard for AC modules.

7. REFERENCES

1. King, D., Boyson, W., Kratochvil, J. (2004). *Photovoltaic Array Performance Model*, SAND2004-3535, Sandia National Laboratories, Albuquerque, NM, December 2004.
2. De Soto, W., Klein, S. A., et al. (2006). *Improvement and Validation of a Model for Photovoltaic Array Performance*. vol. 80, no. 1, pp. 78-88.
3. King, D., Gonzalez, S., et al. (2007). *Performance Model for Grid-Connected Photovoltaic Inverters.* SAND2007-5036, Sandia National Laboratories, Albuquerque, NM, September 2007.
4. Driesse, A., Jain, P., et al. (2008). *Beyond the Curves: Modeling the Electrical Efficiency of Photovoltaic Inverters*. Proc. 33rd IEEE Photovoltaic Specialists Conference, vols. 1-4: 1935-1940.
5. National Fire Protection Association. (2014). NFPA 70: National Electric Code 2014.
6. King, D., Kratochvil, J., Boyson, W. (1997). *Measuring Solar Spectral and Angle-of-Incidence Effects on Photovoltaic Modules and Solar Irradiance Sensors*. Proc. 26th IEEE Photovoltaic Specialist Conference.
7. Riley, D. and Fresquez, A. (2014). *Determining the Effect of Temperature on Microinverter Inversion Efficiency*. Proc. 40th IEEE Photovoltaic Specialist Conference.
8. Luketa-Hanlin, A., and Stein, J., *Improvement and Validation of a Transient Model to Predict Photovoltaic Module Temperature*, SAND2012-4307C, Sandia National Laboratories, Albuquerque, NM, 2012.
9. Neises, T. (2011). *Development and Validation of a Model to Predict the Temperature of a Photovoltaic Cell*, University of Wisconsin-Madison.
10. Kasten, F. and Young, A. (1989). *Revised Optical Air Mass Tables and Approximation Formula*. Applied Optics, vol. 28, Issue 2, pp. 4735-4738.
11. Gueymard, C. *Critical Analysis and Performance Assessment of Clear Sky Solar Irradiance Models using Theoretical and Measured Data*. Solar Energy. vol. 51, No. 2, pp. 121-138.
12. Duffie, John, and William Beckman. *Solar Engineering of Thermal Processes*. 4th ed. Hoboken, NJ: John Wiley & Sons, 2006. pp. 232.
13. American Society of Heating and Air-Conditioning Engineers. ASHRAE standard 93-77.
14. Martin, N. and Ruiz, J. M. (2001). *Calculation of the PV Modules Angular Losses Under Field Conditions by Means of an Analytical Model*. Solar Energy Materials & Solar Cells, vol. 70, pp. 25-38.
15. Erbs, D. G., Klein, S. A., and Duffie, J. A. (1982). *Estimation of the Diffuse Radiation Fraction for Hourly, Daily and Monthly –Average Global Radiation*. Solar Energy. vol. 28, no. 4, pp. 293-302.
16. Boland, J., Ridley, B., and Brown, B. (2008). *Models of Diffuse Solar Radiation*. Renewable Energy. vol. 33, no. 4, pp. 575-584.
17. Reindl, D. T., Beckman, W. A., and Duffie, J. A. (1990). *Diffuse Fraction Correlations*. Solar Energy. vol. 45, no. 1, pp. 1-7.
18. Orgill, J. F. and Hollands, K. G. T. (1977). *Correlation Equation for Hourly Diffuse Radiation on a Horizontal Surface*. Solar Energy. vol. 19, no. 4, pp. 357-359.
19. Maxwell, E. L. (1987). *A Quasi-Physical Model for Converting Hourly Global Horizontal to Direct Normal Insolation*. Solar Energy Research Institute, Tech. Rep.
20. Perez, R. (1992). *Dynamic Global to Direct Conversion Models*. ASHRAE Transactions Research Series, pp. 154-168.

21. Posadillo, R. and López Luque, R. (2009). *Hourly Distributions of the Diffuse Fraction of Global Solar Irradiation in Cordoba (Spain)*. Energy Conversion and Management. vol. 50, no. 2, pp. 223-231
22. Hay, J. and Davies, J. (1980). *Calculations of the Solar Radiation Incident on an Inclined Surface*. Proceedings of First Canadian Solar Radiation Data Workshop, 59. Ministry of Supply Services, Canada.
23. Perez, R. et. al. (1990). *Modeling Daylight Availability and Irradiance Components from Direct and Global Irradiance*. Solar Energy. vol. 44, no. 5, pp. 271-289.
24. Liu, B. Y. H. and Jordan, R. C. (1960). *The Interrelationship and Characteristic Distribution of Direct, Diffuse and Total Solar Radiation*. Solar Energy. vol. 4, no. 3, pp. 1-19.
25. Hansen, C. W., et. al. (2014). *Calibration of Photovoltaic Module Performance Models Using Monitored System Data*. Proceedings of 29th European Photovoltaic Solar Energy Conference and Exhibition. pp. 3472-3476. DOI: 10.4229/EUPVSEC20142014-5DV.3.56
26. Hansen, C. W., et. al. (2014). *Photovoltaic System Model Calibration Using Monitored System Data*. Proceedings of 6th World Conference on Photovoltaic Energy Conversion. Also from Sandia National Laboratories, SAND2014-19650C.
27. Weisstein, Eric W. "Least Squares Fitting--Exponential." From MathWorld--A Wolfram Web Resource. Retrieved Jan. 2015, from http://mathworld.wolfram.com/LeastSquaresFittingExponential.html
28. Moler, C (2013). The Lambert W Function. *Cleve's Corner* [web log]. Retrieved Dec. 2014, from http://blogs.mathworks.com/cleve/2013/09/02/the-lambert-w-function/

DISTRIBUTION

1	MS0951	Bruce King	Org. 6112
1	MS1033	Abe Ellis	Org. 6112
1	MS0899	Technical Library	9536 (electronic copy)


Sandia National Laboratories